Modelarea cu Ordin Redus a Curgerilor in Turbomasini

Paul Cizmas
Department of Aerospace Engineering
Texas A&M

Planul Prezentarii

- Introducere
  - Background si Necesitatea Cercetarii
- Exemple de Curgeri Nestationare
- Modele pentru Curgeri Nestationare
  - Time Linearization
  - Harmonic Balance
  - Reduced-Order Models
  - Volterra Series
- Proper Orthogonal Decomposition
  - Metode de Accelerare
- Concluzii

Background

- Challenges
  - Turbomachinery is the test bed for unsteady aerodynamics
  - Governing equations for unsteady aerodynamics are sets of large PDEs that change character depending on flow conditions
  - While ODEs solvers are widely available, this is not the case for PDEs; PDE solvers are few and cover a narrow range of applications
  - Numerical solutions of PDEs boil down to solving a different set of equations after discretization
  - There is no "*faithful solution*" to PDEs
- Implication
  - Computational time is extremely large for high-fidelity models

Background

- Need for Unsteady Aerodynamics
  - Performance
    - Compressor and Turbine Airfoil Indexing
    - Axial Thrust Prediction in Centrifugal Compressors
  - Aero-Mechanics
    - Flow Control for Suppressing Rotating Stall
    - Fluid Instabilities in Honeycomb Stator Seals
    - Continuation/POD method for Turbomachinery Aeroelastic Analysis
  - Novel Cycles
    - In-Situ Reheat and Turbine-Combustors

Compressor and Turbine Airfoil Indexing

- New design expected efficiency increase 0.3-0.5 points
- Old design with airfoil indexing - up to 2 points

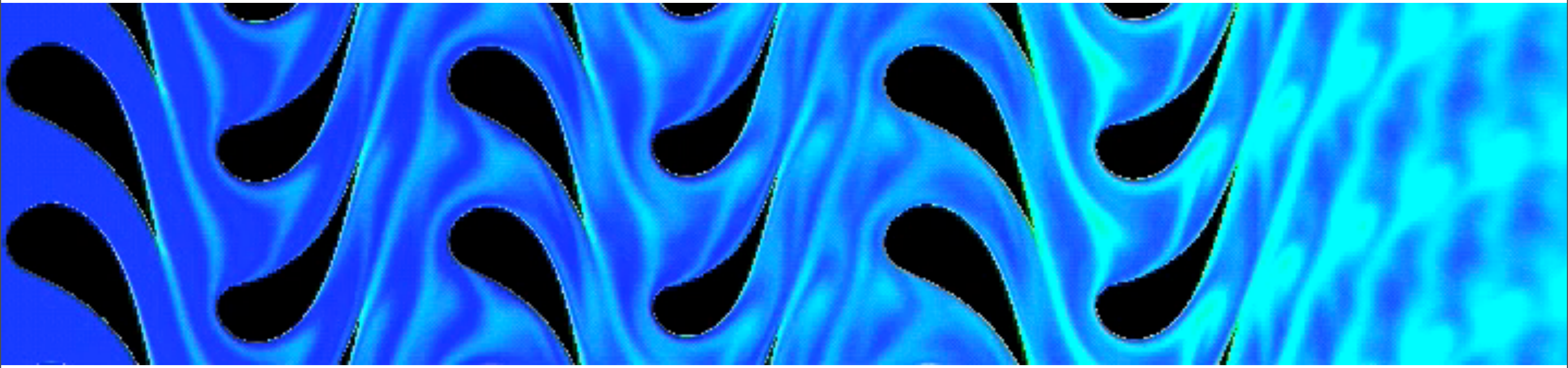

- Multi-row interaction

potential flow interaction	shock-boundary layer interaction
wake interaction	hot streak interaction
vortex shedding	flutter

PaRSI

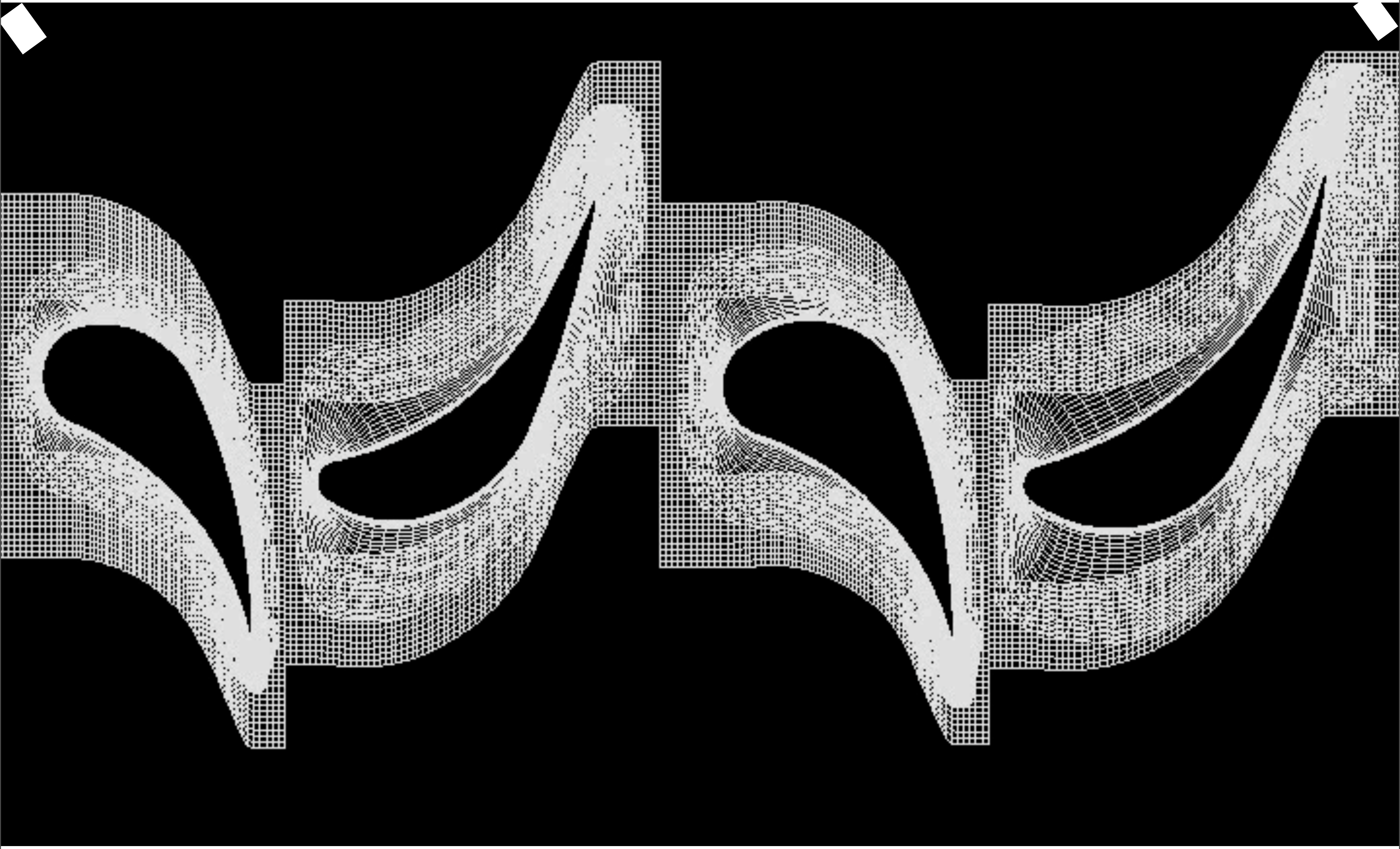

PaRSI

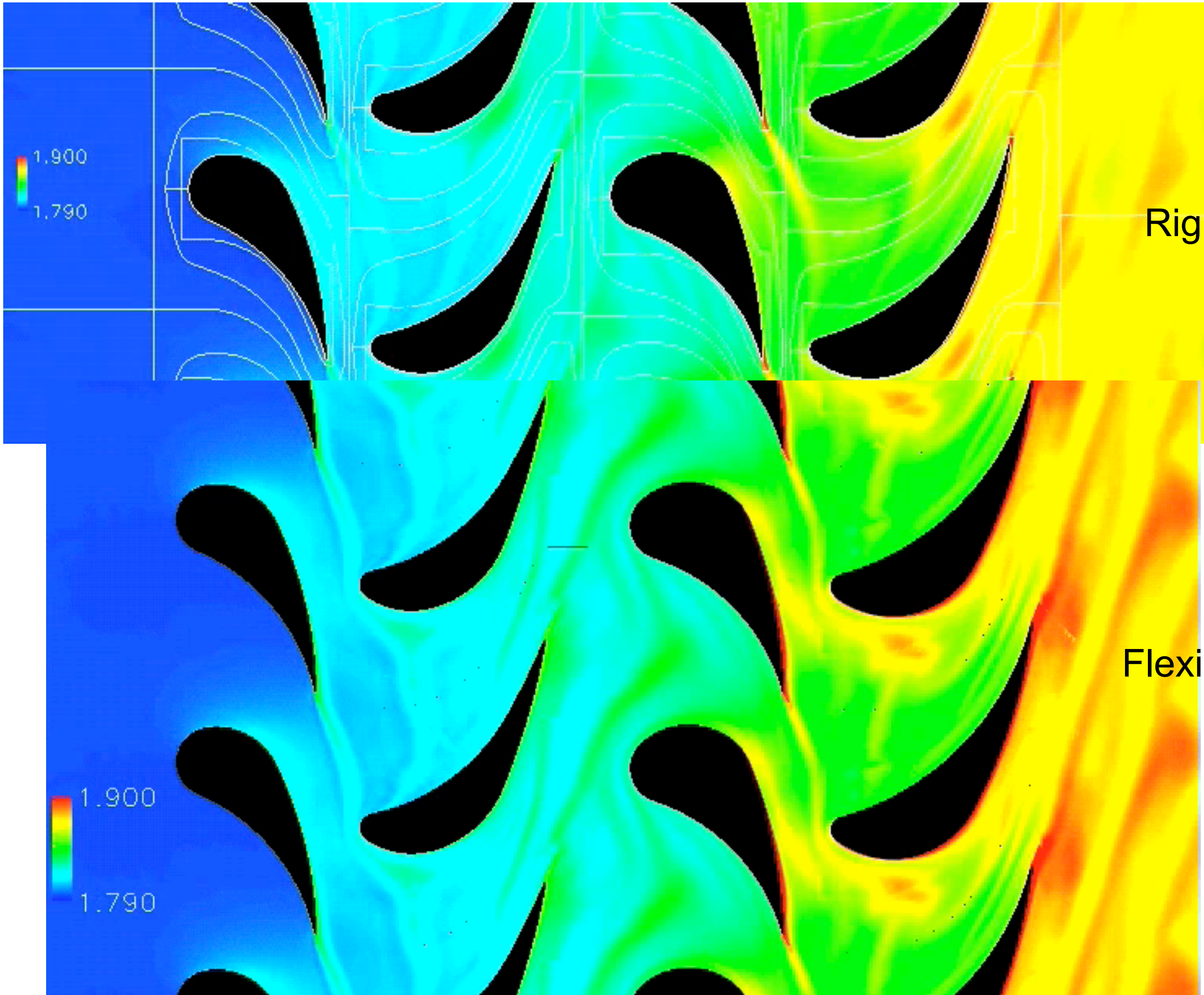

In-Situ Reheat and Turbine-Combustors

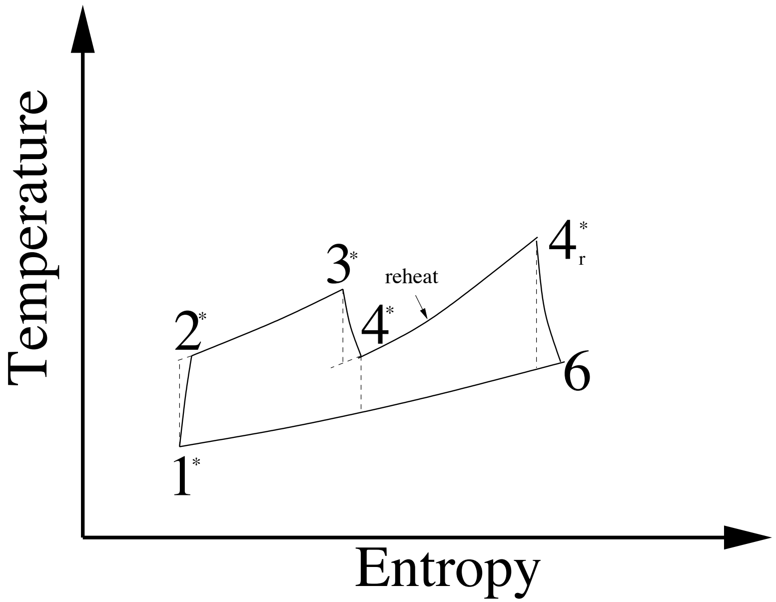

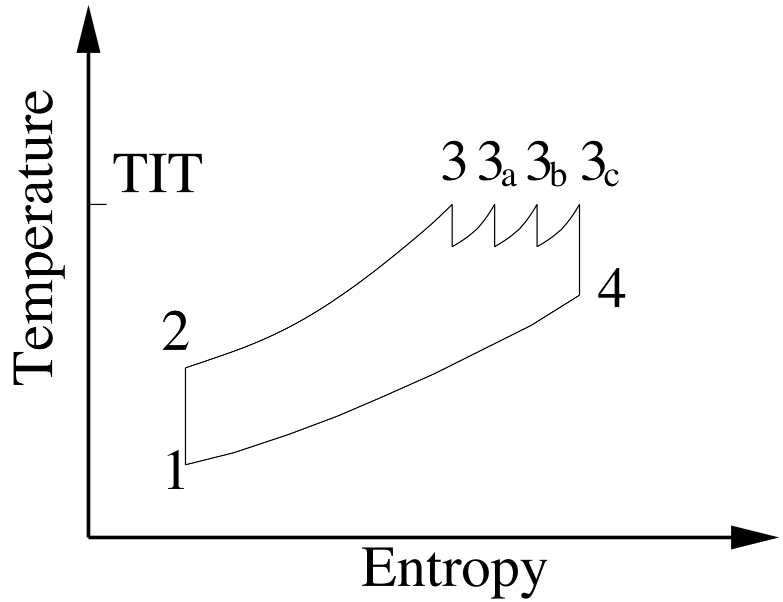

O2 mass fraction

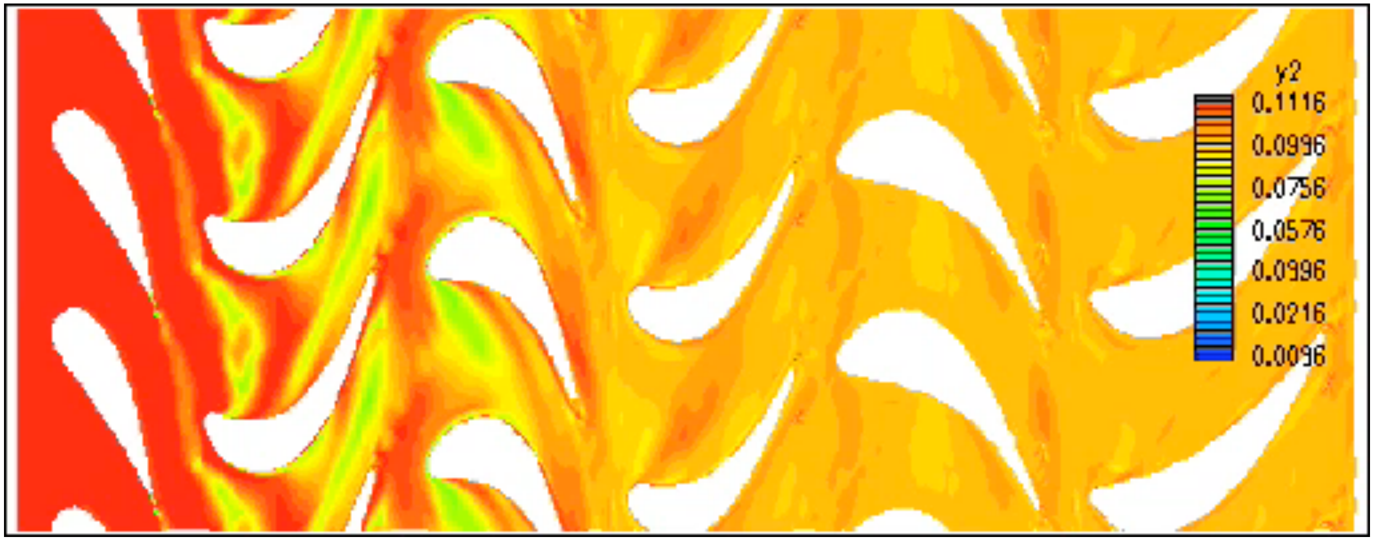

Axial Thrust Prediction in Centrifugal Compressors

- Prior one could not even predict the sign of axial thrust!

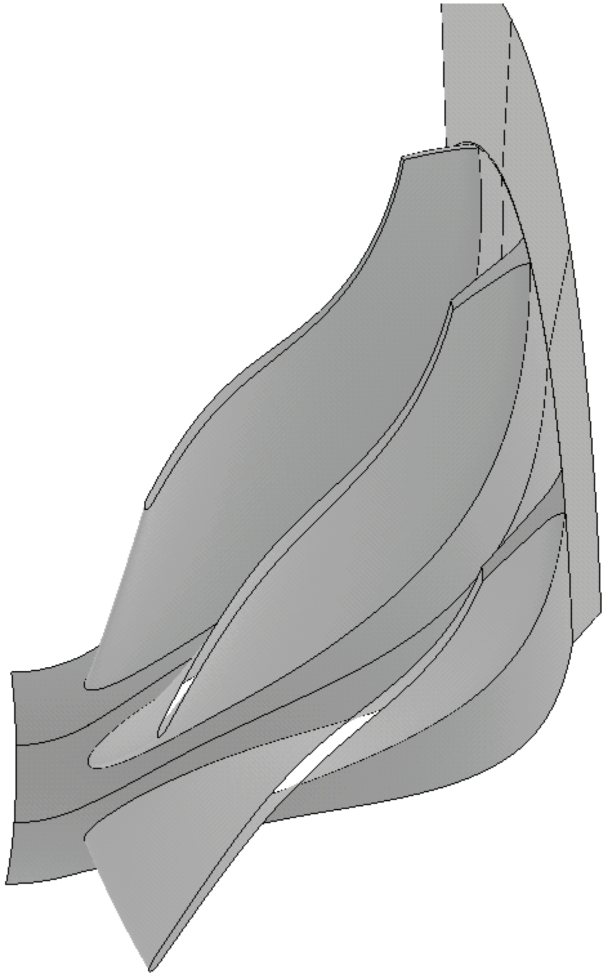

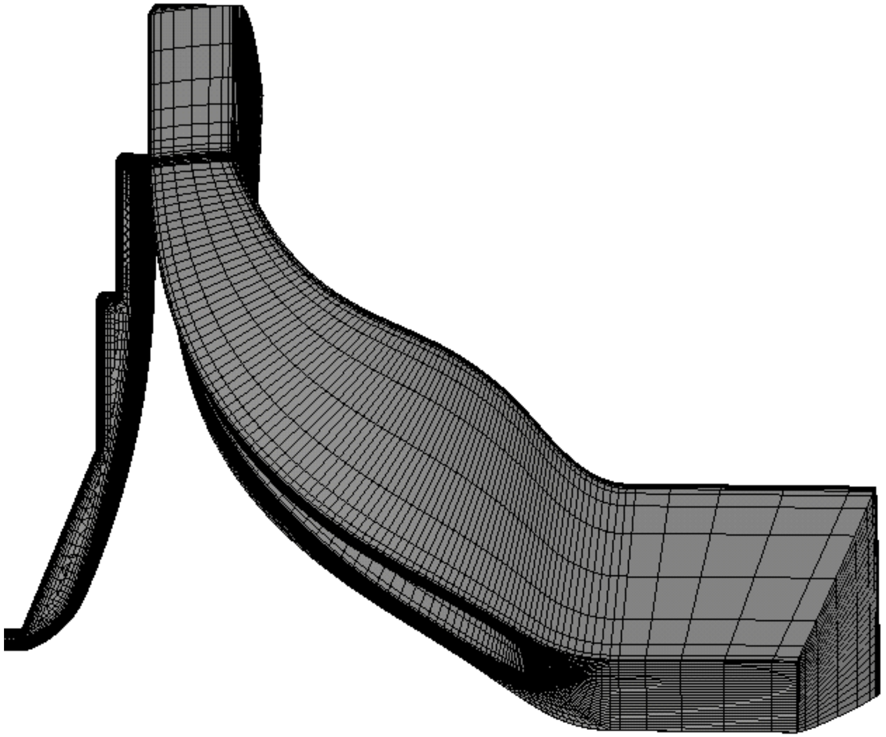

Axial Thrust Prediction

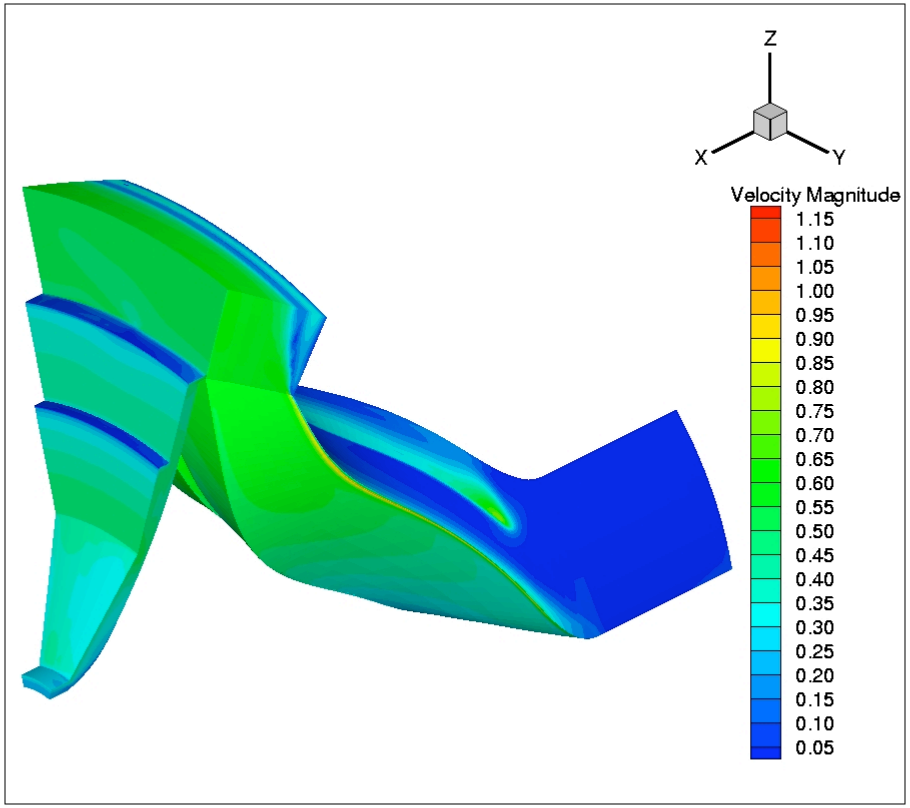

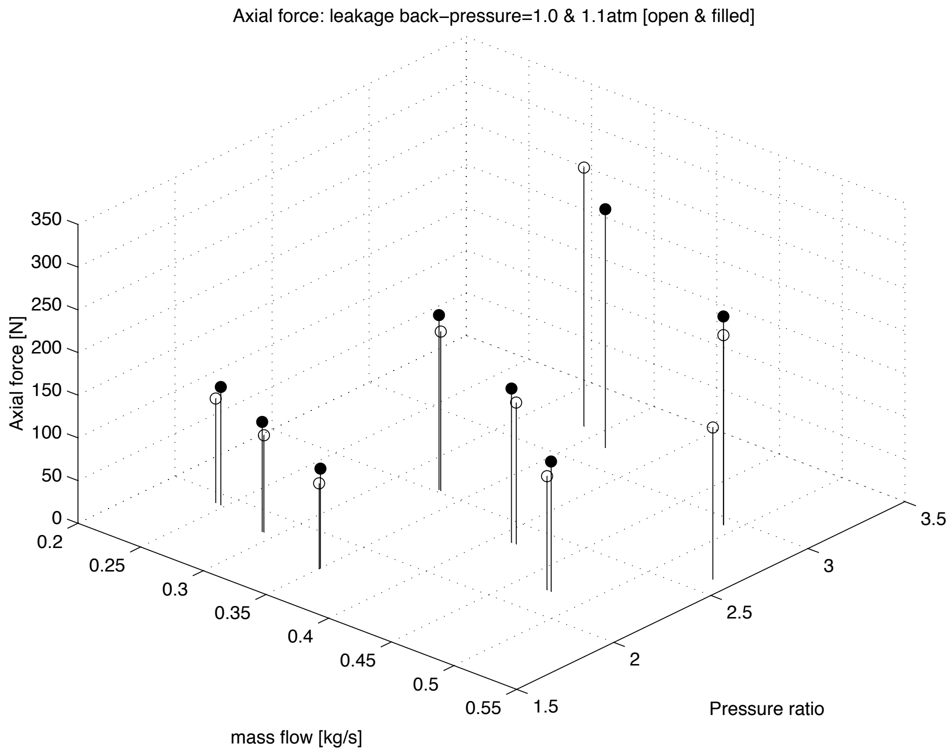

UNS3D
Serpentine Jet Engine Inlet Duct

	Experiment [m]	Fluent [m]	UNS3D [m]	Fluent Error [%]	UNS3D Error [%]
First bend	0.3302	0.403	0.339	22.05	2.66
Second bend	0.602	0.591	0.601	-1.83	-0.17

UNS3D

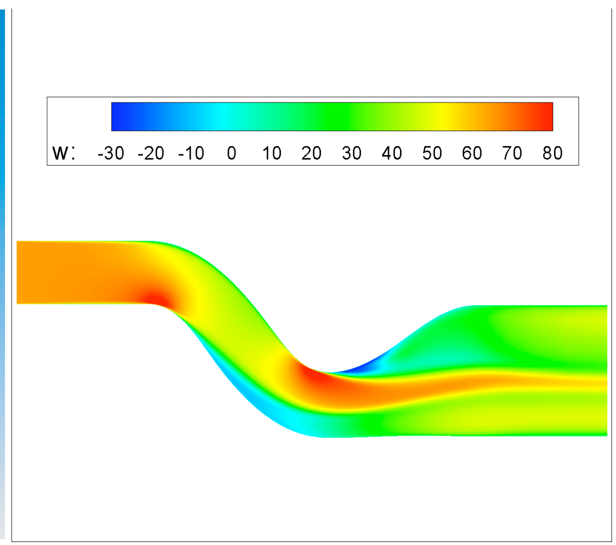

Fluent

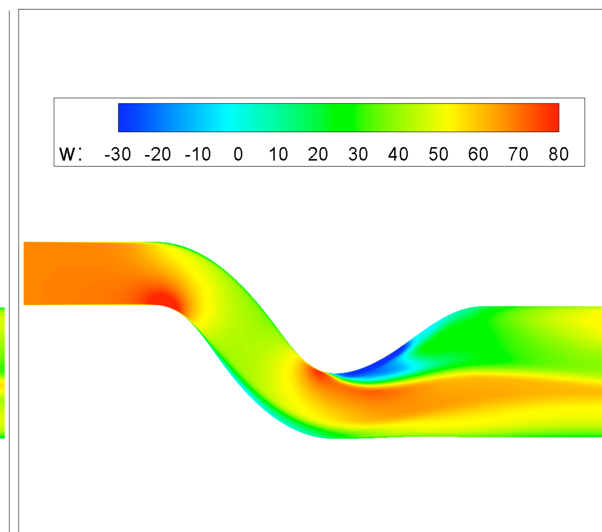

Flow Control for Suppressing Rotating Stall

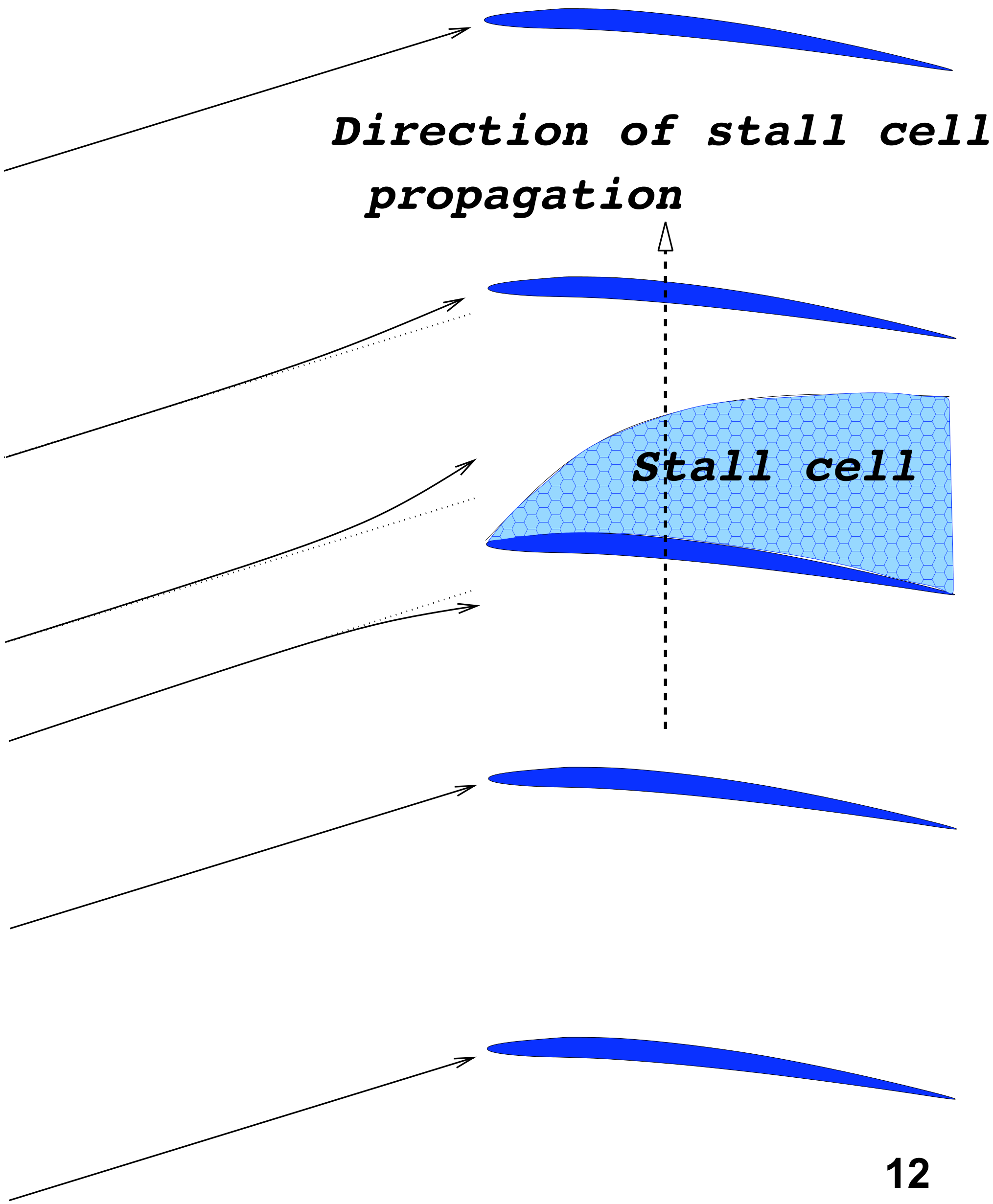

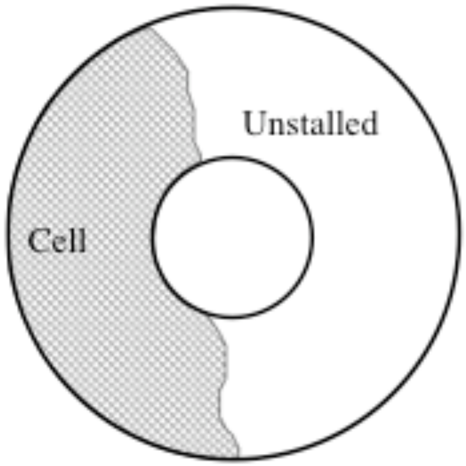

Full−span stall

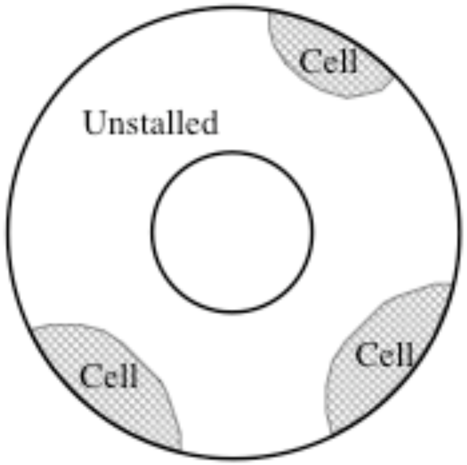

Part−span stall (three cells)

Flow Control for Suppressing Rotating Stall

Approach
Key Ingredients

Super-blade

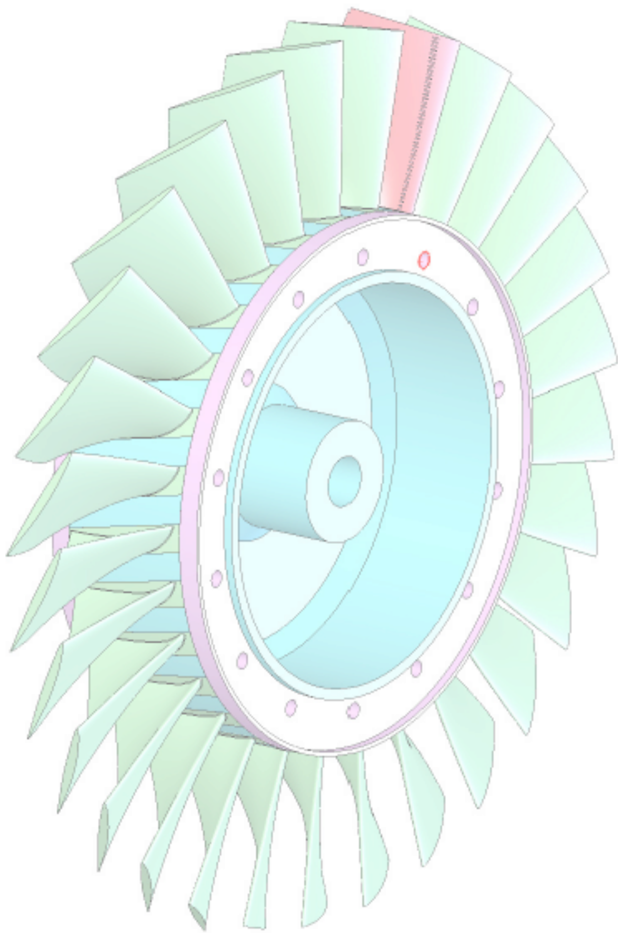

Pulsing modulator

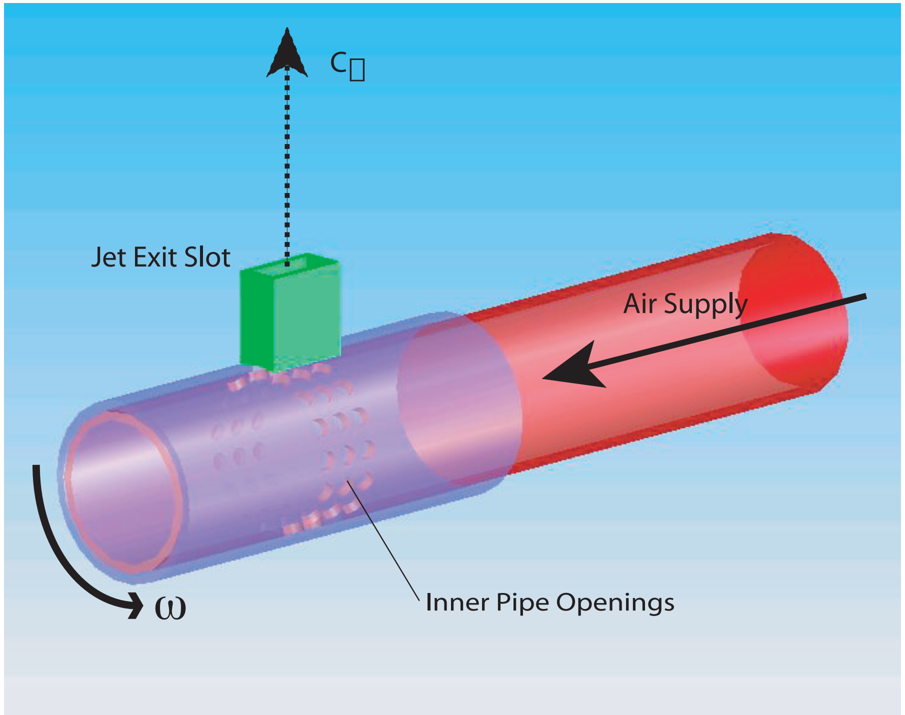

Fluid Instabilities in Hole Pattern and Honeycomb Stator Seals

Density contour plots: unbounded (left), channel flow (right)

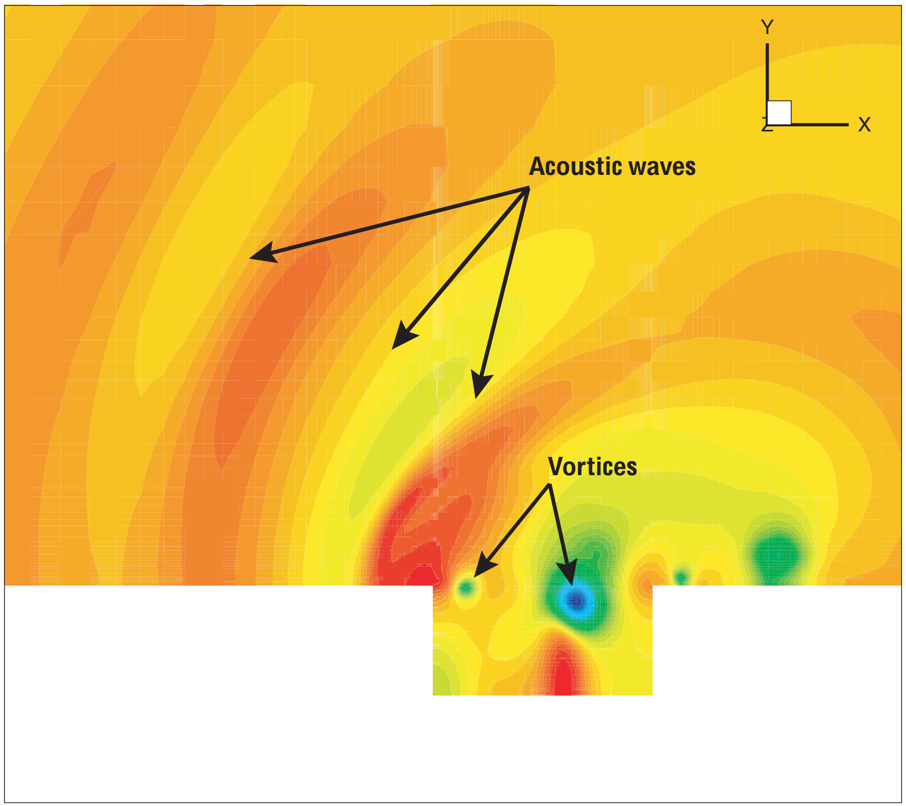

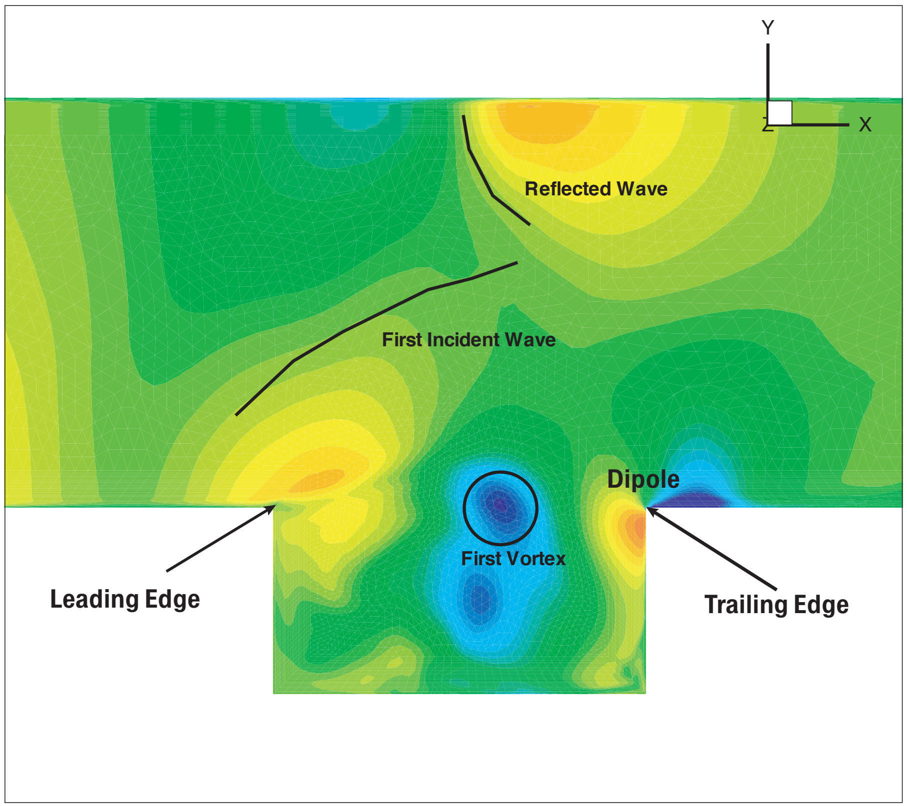

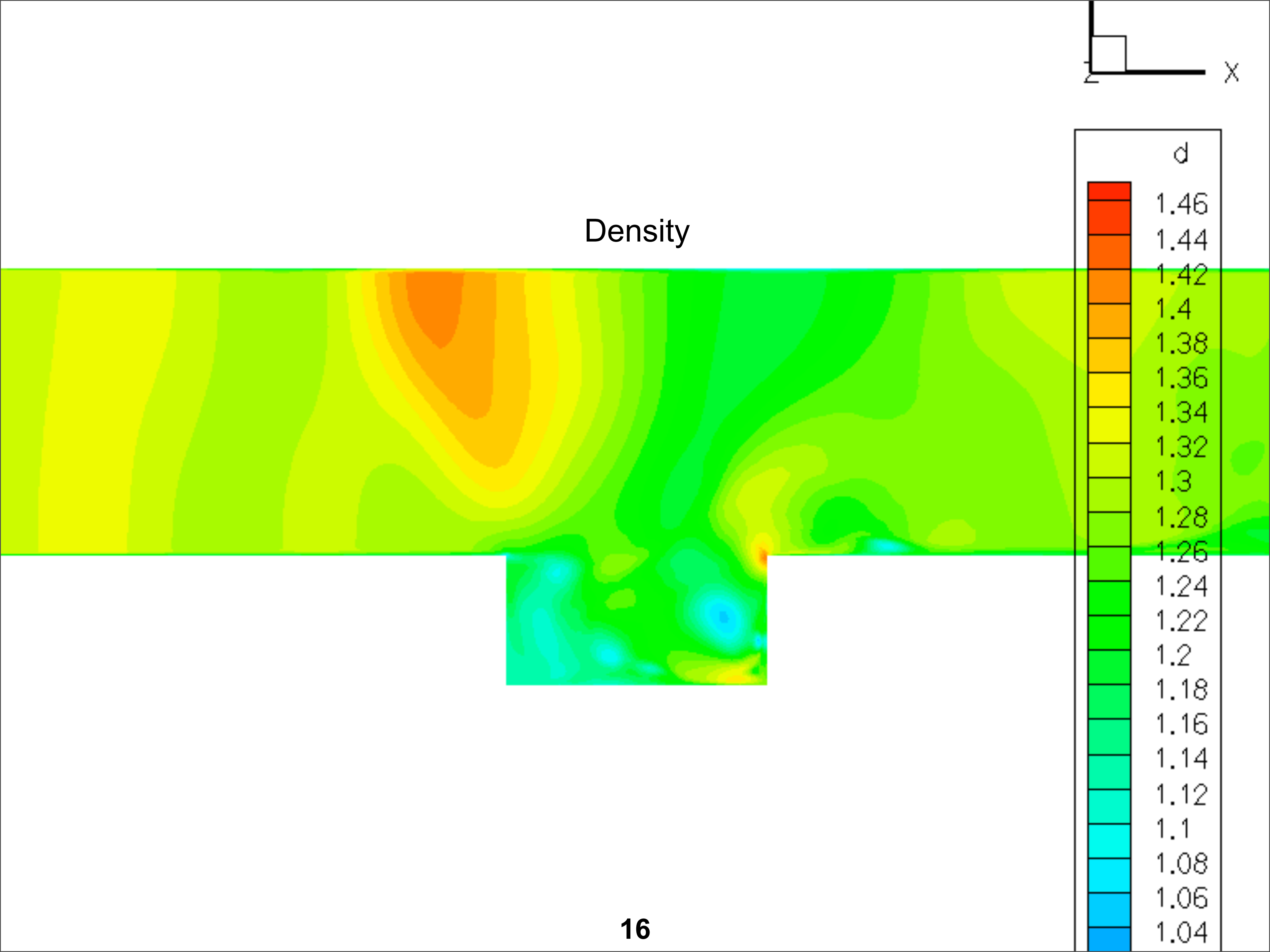
Density
X
d
1.46
1.44
1.42
1.4
1.38
1.36
1.34
1.32
1.3
1.28
1.26
1.24
1.22
1.2
1.18
1.16
1.14
1.12
1.1
1.08
1.06
1.04

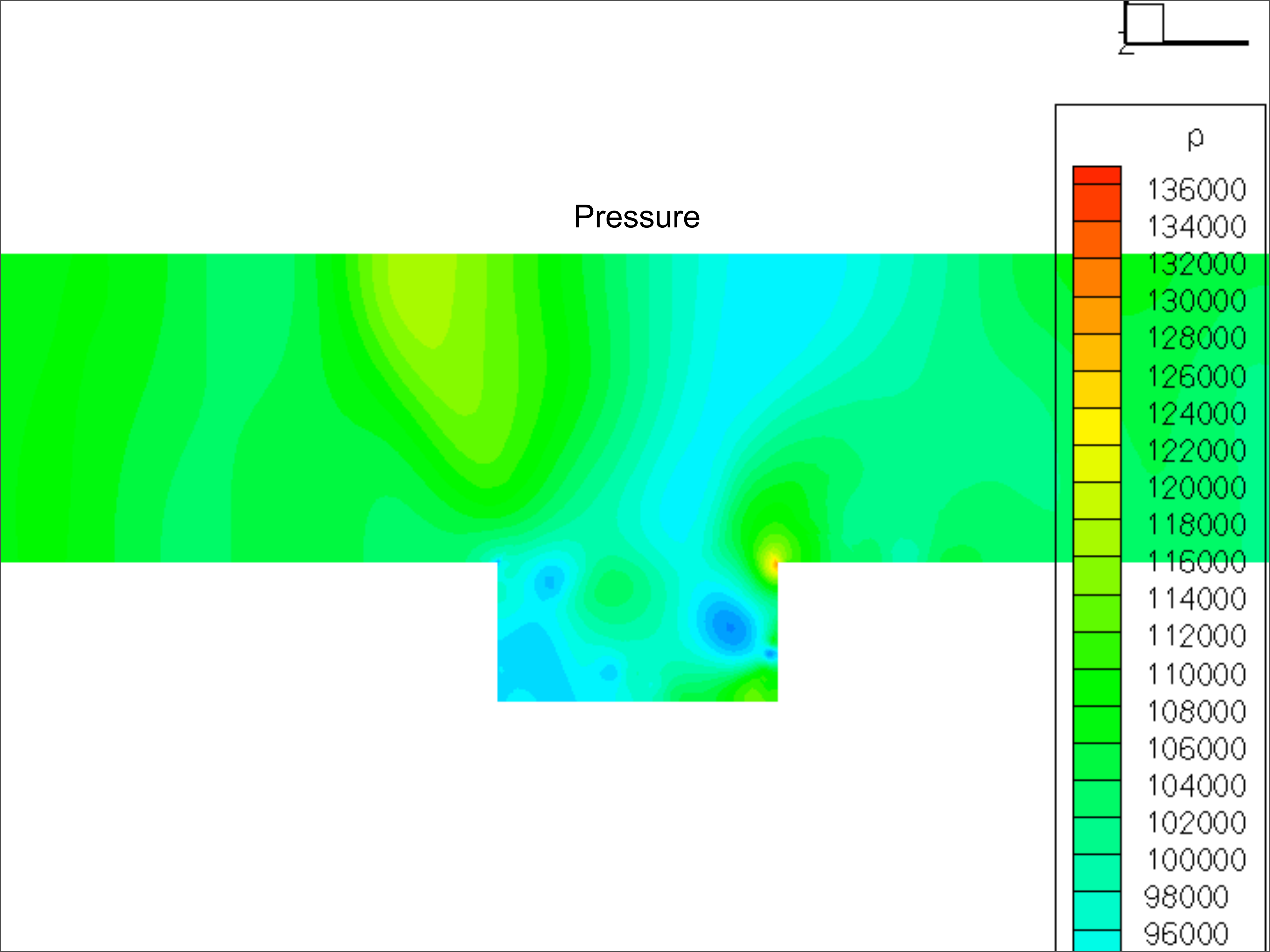

Pressure
p
136000
134000
132000
130000
128000
126000
124000
122000
120000
118000
116000
114000
112000
110000
108000
106000
104000
102000
100000
98000
96000

Flow Analysis Tools

- Parallel Rotor-Stator Interaction (PaRSI)
- Unsteady Unstructured 3D (UNS3D)
- Grid Generator (GG)
- Combustion and Rotor-Stator Interaction (CoRSI)
- PaRSI/POD

Unsteady Aerodynamic Models

- Time linearization
- Harmonic balance (HB)
- Proper orthogonal decomposition (POD)
- Volterra series (VS) and transfer (or describing) functions

---

- Only HB, POD and VS capture nonlinearities
- HB requires flow be periodic in time
- VS limited by convergence issues and need high-order kernels

Time linearization

- Small (linear) dynamic perturbation about a (nonlinear) mean flow
  - Time domain
  - Frequency domain
- Pros:
  - Computationally very inexpensive
  - Good for linear stability of AE system
- Cons:
  - Cannot capture nonlinearities
  - Cannot determine LCO amplitude

Harmonic Balance

- Assumes flow is periodic & expands in terms of a Fourier series in time
- Retains physical dimensions of a full-order model
- Transforms from time domain to frequency domain
- Pros:
  - Number of harmonic frequencies << time steps
- Cons:
  - Flow must be periodic in time

Reduced-Order Models

- Determine dominant spatial modes & use these modes to represent the flow
- Proper Orthogonal Decomposition offers best approximation for *any* number of modes

Volterra Series & Transfer Functions

- Volterra series in time domain
- Transfer functions (or describing functions for nonlinear case) in frequency domain
- Pros:
  - Generate small computational models from large CFD data sets
- Cons:
  - Approach more developed for dynamically linear case

POD Method

Extracts:

– time-independent orthonormal basis functions $\Phi_k(x)$

– time-dependent orthonormal amplitude coefficients $a_k(t_i)$

such that the reconstruction

$$u(\mathbf{x}, t_i) = \sum_{k=1}^{M} a_k(t_i)\, \Phi_k(\mathbf{x}), \quad i = 1, \ldots, M$$

is optimal in the sense that the average least square truncation error

$$\varepsilon_m = \left\langle \left\| u(\mathbf{x}, t_i) - \sum_{k=1}^{m} a_k(t_i)\, \Phi_k(\mathbf{x}) \right\|^2 \right\rangle$$

is a minimum for any given number $m \leq M$ of basis functions over all possible sets of orthogonal functions

POD Method

Optimal property (1) reduces to

$$\int_D < u(x)u^*(y) > \Phi(y)dy = \lambda\Phi(x) \qquad (2)$$

$\{\Phi_k\}$ are eigenfunctions of integral equation (2), whose kernel is the averaged autocorrelation function

$$< u(x)u^*(y) > \equiv R(x,y) \qquad (3)$$

For a finite-dimensional case, (3) replaced by tensor product matrix

$$R(\mathbf{x},\mathbf{y}) = \frac{1}{M}\sum_{i=1}^{M} u(\mathbf{x},\, t_i)\, u^T(\mathbf{y}, t_i)$$

POD Method

Features

- Provides optimal basis for modal decomposition of a data set
- Extracts key *spatial* features from physical systems with spatial and temporal characteristics
- Reduces a large set of governing PDEs to a much smaller of ODEs

Steps

- Database generation
- Modal decomposition
- Galerkin projection
- Time coefficients computation

POD Method

Full-order model governing equations

$$\frac{\partial}{\partial t}(\epsilon_m \rho_m) + \nabla \cdot (\epsilon_m \rho_m \vec{v}_m) = 0$$

$$\frac{\partial}{\partial t}(\epsilon_m \rho_m \vec{v}_m) + \nabla \cdot (\epsilon_m \rho_m \vec{v}_m \vec{v}_m) = -\epsilon_m \nabla p_g + \nabla \cdot \overline{\overline{S}}_m + F_{gs}(\vec{v}_s - \vec{v}_g) + \epsilon_m \rho_m \vec{g}$$

$$\epsilon_m \rho_m C_{p_m} \left(\frac{\partial T_m}{\partial t} + \vec{v}_m \nabla T_m \right) = -\nabla \vec{q}_m - \gamma_m (T_m - T_\ell) - \Delta H_{rm} + \gamma_{Rm}(T_{Rm}^4 - T_m^4)$$

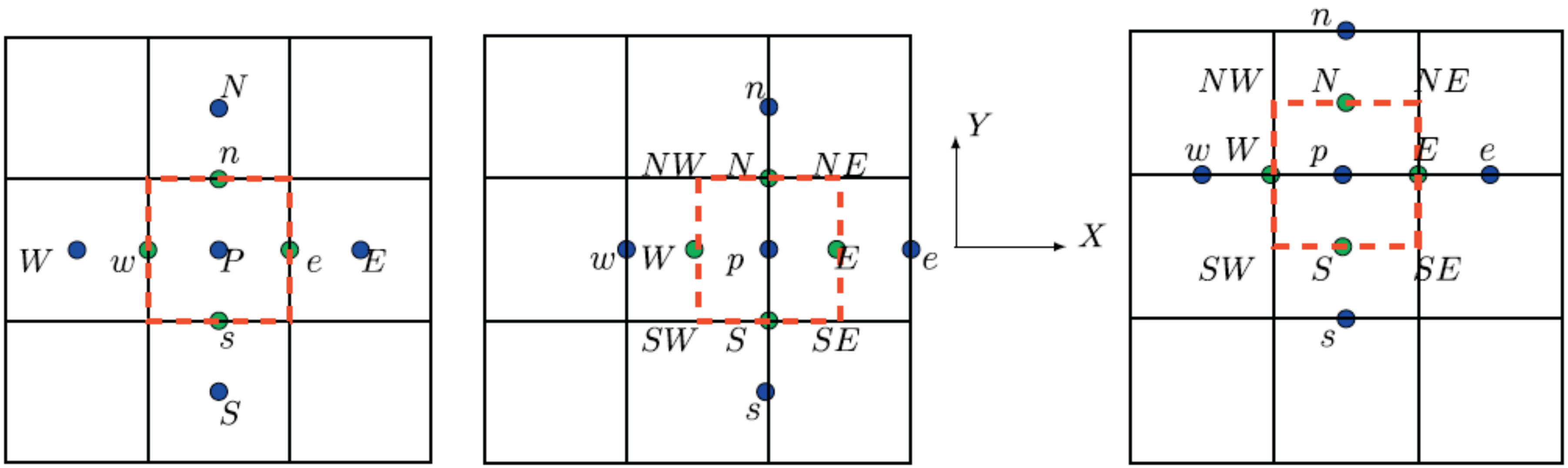

POD Method

$$(a^v_m)_p(v_m)_p = \sum_{nb}(a^v_m)_{nb}(v_m)_{nb} + (b^v_m)_p$$

$$v(x,t) = \sum_{k=1}^{m^v} \alpha^v_k(t)\varphi^v_k(x)$$

$$\sum_{k=1}^{m} \alpha_k \left(a_i\varphi_k(x_i) - \sum_{i_{nb}=1}^{NB} a_{i_{nb}}\varphi_k(x_{i_{nb}}) \right) = b_i, \qquad i = 1,\ldots,N$$

$$\sum_{k=1}^{m} \alpha_k \left([A]\{\varphi_k\} - \sum_{nb=1}^{NB} [A_{nb}]\{\varphi_{k_{nb}}\} \right) = \{b\}$$

$$\{\varphi_\ell\}^T \sum_{k=1}^{m} \alpha_k \left([A]\{\varphi_k\} - \sum_{nb=1}^{NB} [A_{nb}]\{\varphi_{k_{nb}}\} \right) = \{\varphi_\ell\}^T\{b\}, \qquad \ell = 1,\ldots,m$$

$$\left[\tilde{\mathcal{A}}^v\right]\{\alpha^v\} = \left\{\tilde{\mathcal{B}}^v\right\}$$

Proper Orthogonal Decomposition

- Acceleration methods
  - Database splitting
  - Quasi-symmetrical matrix solver
  - Time step adjustment strategy
  - Updating matrix of time coefficients strategy
  - Sampling strategy

Quasi-symmetry of A Matrix

A matrix for v-velocity

$$\tilde{\mathcal{A}} = \begin{vmatrix} 196.4486 & 63.3060 & 6.0469 & 0.5038 & -21.3047 & 11.9071 & 2.3488 & -6.8064 \\ 63.3060 & 903.4807 & -44.1690 & 6.3410 & 14.0286 & -7.4939 & 6.1636 & 19.8724 \\ 6.0459 & -44.1687 & 243.2099 & -20.7951 & -164.8536 & 68.0529 & 19.3275 & -42.8377 \\ 0.5039 & 6.3411 & -20.7953 & 930.9194 & 31.0348 & 20.0166 & 14.3861 & 15.2768 \\ -21.3042 & 14.0288 & -164.8535 & 31.0347 & 890.8742 & 32.1664 & 42.8224 & -23.8698 \\ 11.9068 & -7.4940 & 68.0527 & 20.0167 & 32.1663 & 904.3555 & -10.8230 & 26.7999 \\ 2.3477 & 6.1634 & 19.3267 & 14.3861 & 42.8222 & -10.8228 & 872.6460 & 92.5161 \\ -6.8042 & 19.8722 & -42.8362 & 15.2768 & -23.8695 & 26.7996 & 92.5161 & 763.9839 \end{vmatrix}$$

$$\tilde{\mathcal{A}}_{\ell k}^{\epsilon_s} = \{\varphi_\ell\}^T [A]\{\varphi_k\} - \sum_{nb=1}^{NB} \{\varphi_\ell\}^T [A_{nb}]\{\varphi_{k_{nb}}\}, \qquad \ell, k = 1, \ldots, m$$

Algorithm for solving quasi-symmetrical matrices

$$Ax = b$$

$$(A_s + A_n)x = b$$

$$A_s x_s^{(1)} = b$$

$$x = x_s^{(1)} + x_n^{(1)}$$

$$(A_s + A_n)x_n^{(i)} = -A_n x_s^{(i)}$$

$$x_n^{(i)} = x_s^{(i+1)} + x_n^{(i+1)}$$

$$x = x_s^{(1)} + x_s^{(2)} + \cdots + x_s^{(m)} + x_n^{(m)}$$

Note : A_n can be chosen such that to reduce number of operations in $-A_n x_s^{(\ell)}$

Algorithm for solving quasi-symmetrical matrices

1. For given A, find A_n and A_s
2. For given A_s, find L where $LL^T=A_s$
3. For given L and b, find $x_s^{(1)}$
4. For given $x_s^{(1)}$ and A_n find $b^{(1)}$
5. Repeat steps 3 and 4 until $x_s^{(m)}$ is smaller than a given error

Splitting Matrix A

Split 1

$$A_s = \begin{bmatrix} a_{11} & a_{21} & \dots & a_{m1} \\ a_{21} & a_{22} & \dots & a_{m2} \\ \vdots & \vdots & & \vdots \\ a_{m1} & a_{m2} & \dots & a_{mm} \end{bmatrix}$$

$$A_n = \begin{bmatrix} 0 & a_{12} - a_{21} & \dots & a_{1m} - a_{m1} \\ 0 & 0 & \dots & a_{2m} - a_{m2} \\ \vdots & \vdots & & \vdots \\ 0 & 0 & \dots & 0 \end{bmatrix}$$

Split 2

$$A_s = \frac{1}{2}(A + A^T)$$

$$A_n = \frac{1}{2}(A - A^T)$$

	Split 1			Split 2		
	$x_s^{(1)}$	$x_s^{(2)}$	$x_s^{(3)}$	$x_s^{(1)}$	$x_s^{(2)}$	$x_s^{(3)}$
1	0.2205E+00	-0.5529E-06	0.7659E-12	0.2205E+00	-0.3159E-06	-0.3772E-11
2	-0.1401E+00	0.3505E-07	-0.1631E-12	-0.1401E+00	0.4948E-07	0.2289E-12
3	0.3053E-01	-0.2586E-06	-0.3920E-12	0.3053E-01	0.3431E-06	-0.2669E-11
4	-0.4188E-01	-0.1645E-07	0.8489E-14	-0.4188E-01	0.1406E-07	0.5404E-14
5	0.3669E-01	-0.8025E-07	-0.6626E-13	0.3669E-01	-0.2367E-07	-0.6342E-12
6	-0.4223E-01	0.4975E-07	0.3221E-13	-0.4223E-01	0.4024E-07	0.3478E-12
7	0.5685E-01	0.1344E-07	0.1147E-13	0.5685E-01	0.1726E-06	0.6542E-13
8	-0.1916E-01	-0.2588E-07	-0.1567E-13	-0.1916E-01	-0.4003E-06	-0.9619E-13

Degree of Non-symmetry

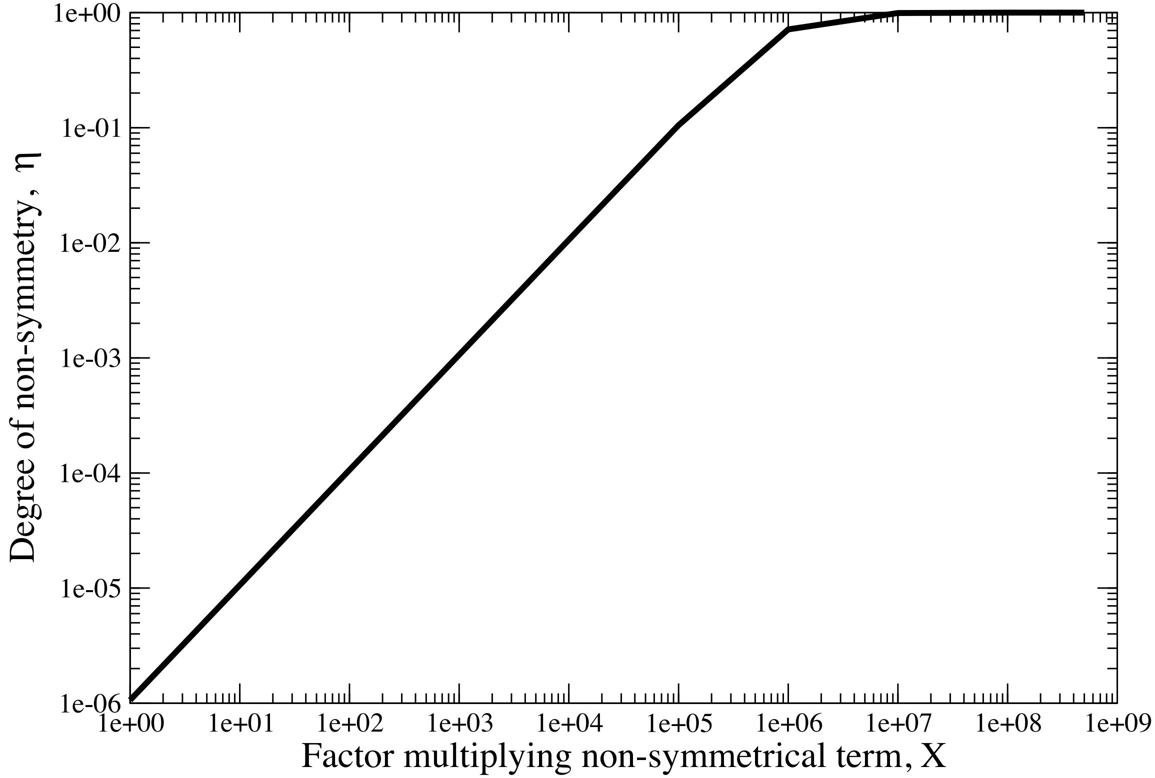

$$\eta = ||A - A^T||_F / ||A + A^T||_F$$

Frobenius (Hilbert-Schmidt) Norm

$$||A||_F = \sqrt{\sum_{i=1}^{m} \sum_{j=1}^{n} |a_{ij}|^2}$$

Effect of Degree of Non-symmetry

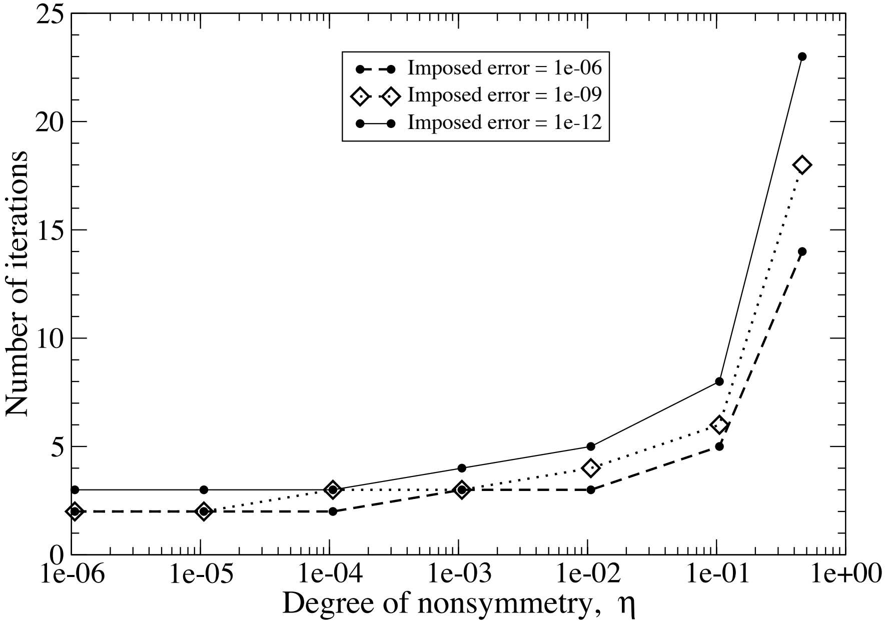

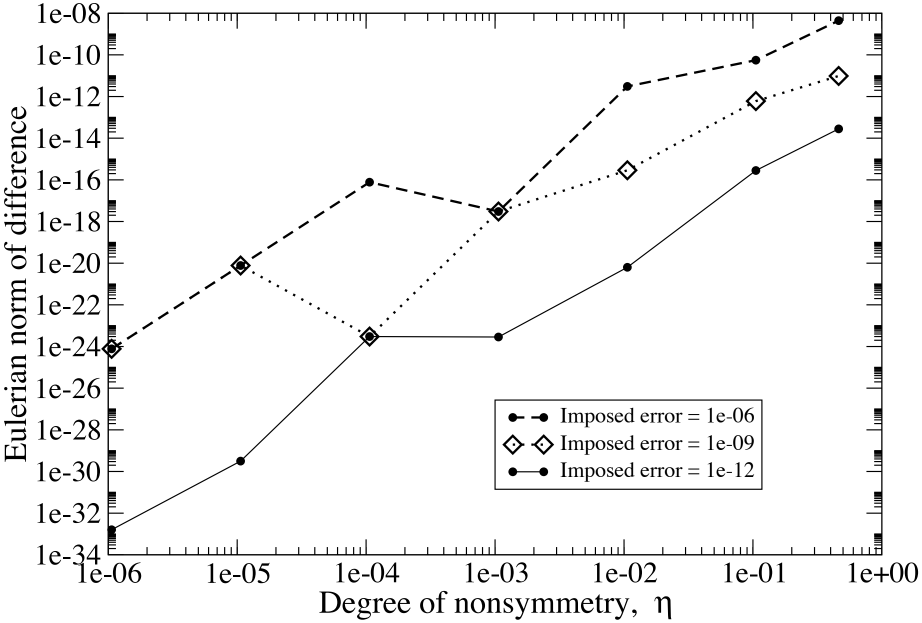

Number of iterations

Eulerian norm of difference between solutions of the LU decomposition and the present method

POD for Turbomachinery Aeroelastic Analysis

A reduced-order model is not necessarily a low-fidelity solution!

Full-Order Model

Reduced-Order Model, POD 40 modes

POD for Turbomachinery Aeroelastic Analysis

A reduced-order model is not necessarily a low-fidelity solution!

Full-Order Model

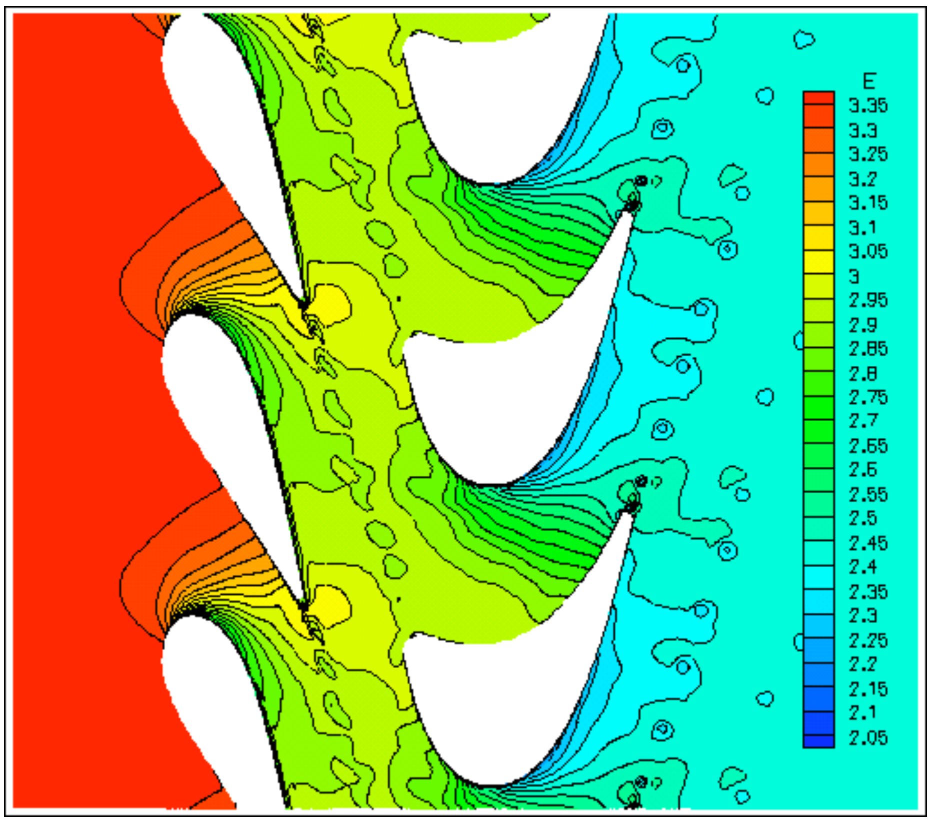

Reduced-Order Model, POD 40 modes

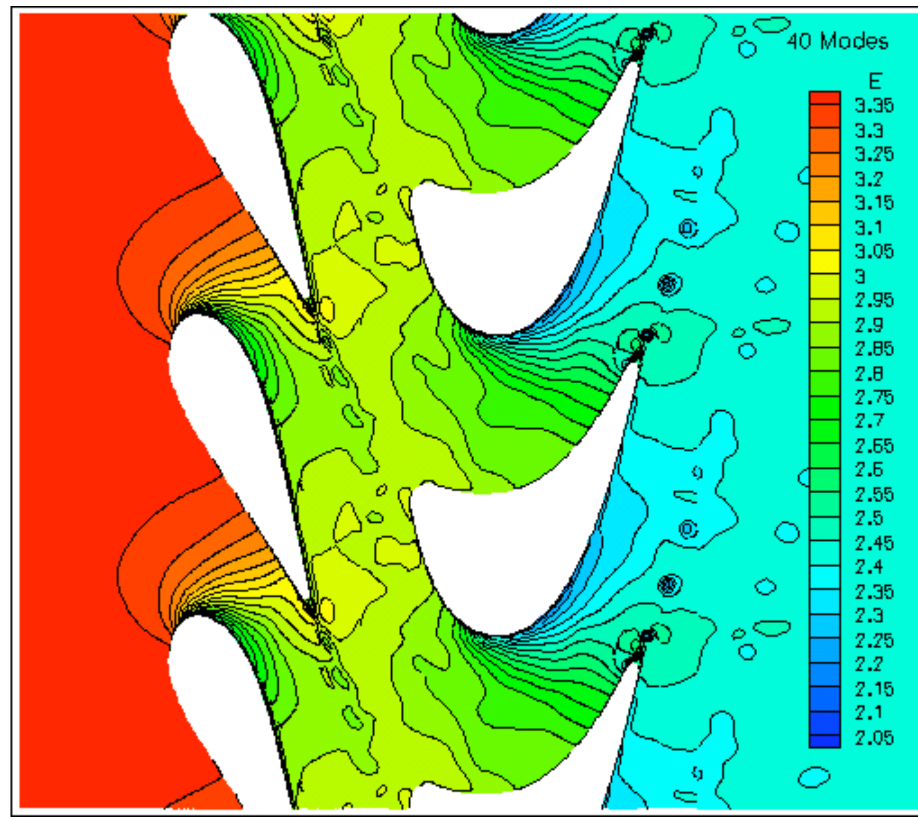

POD for Turbomachinery Aeroelastic Analysis

A reduced-order model is not necessarily a low-fidelity solution!

Full-Order Model

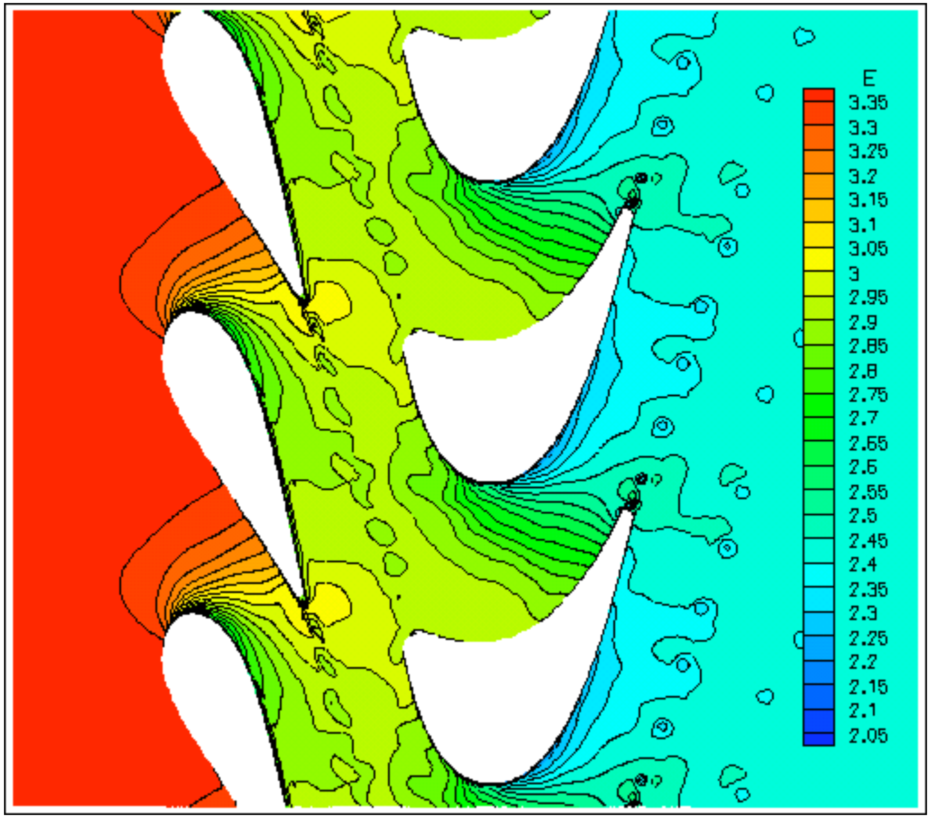

Reduced-Order Model, POD 40 modes

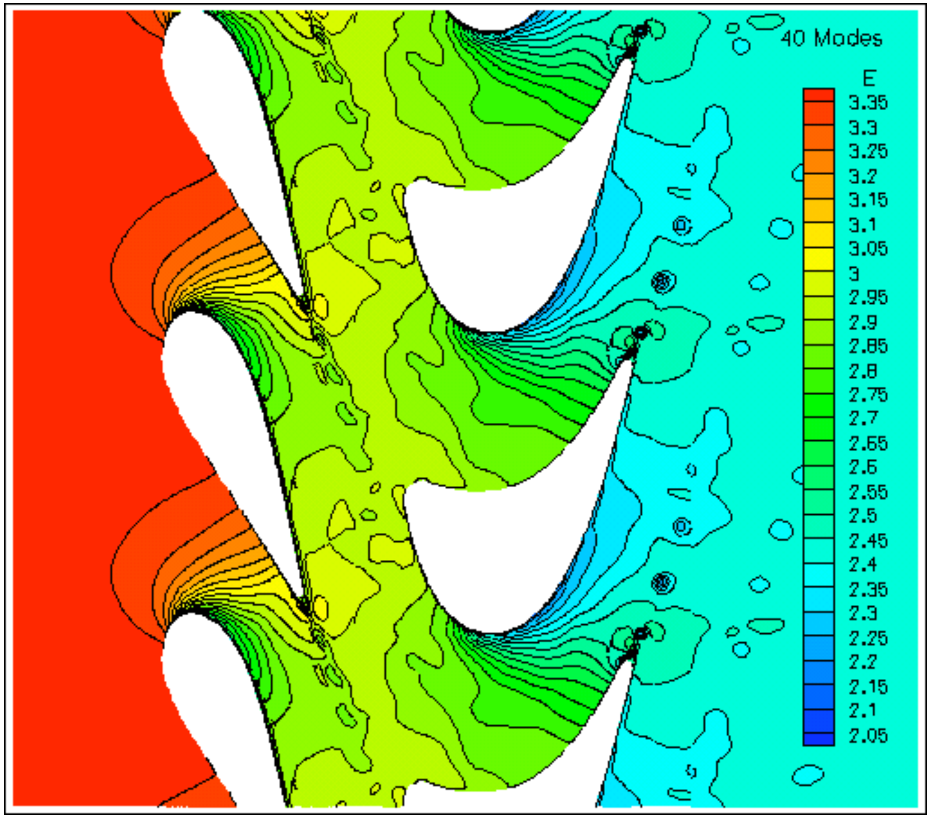

ODEx - POD for Two-Phase Flows

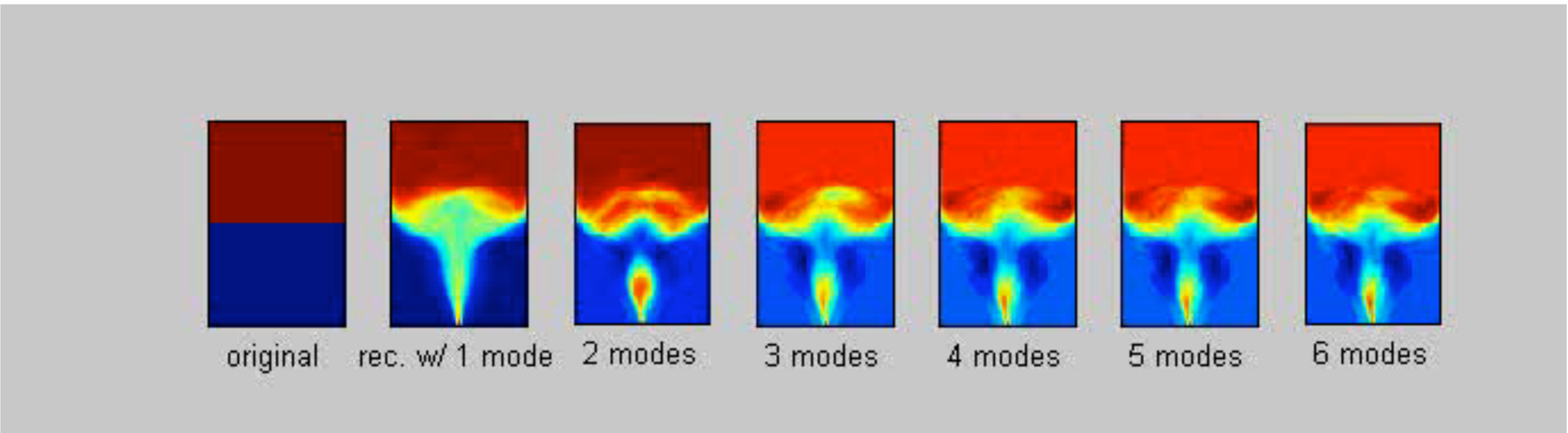

ODEx - POD for Two-Phase Flows

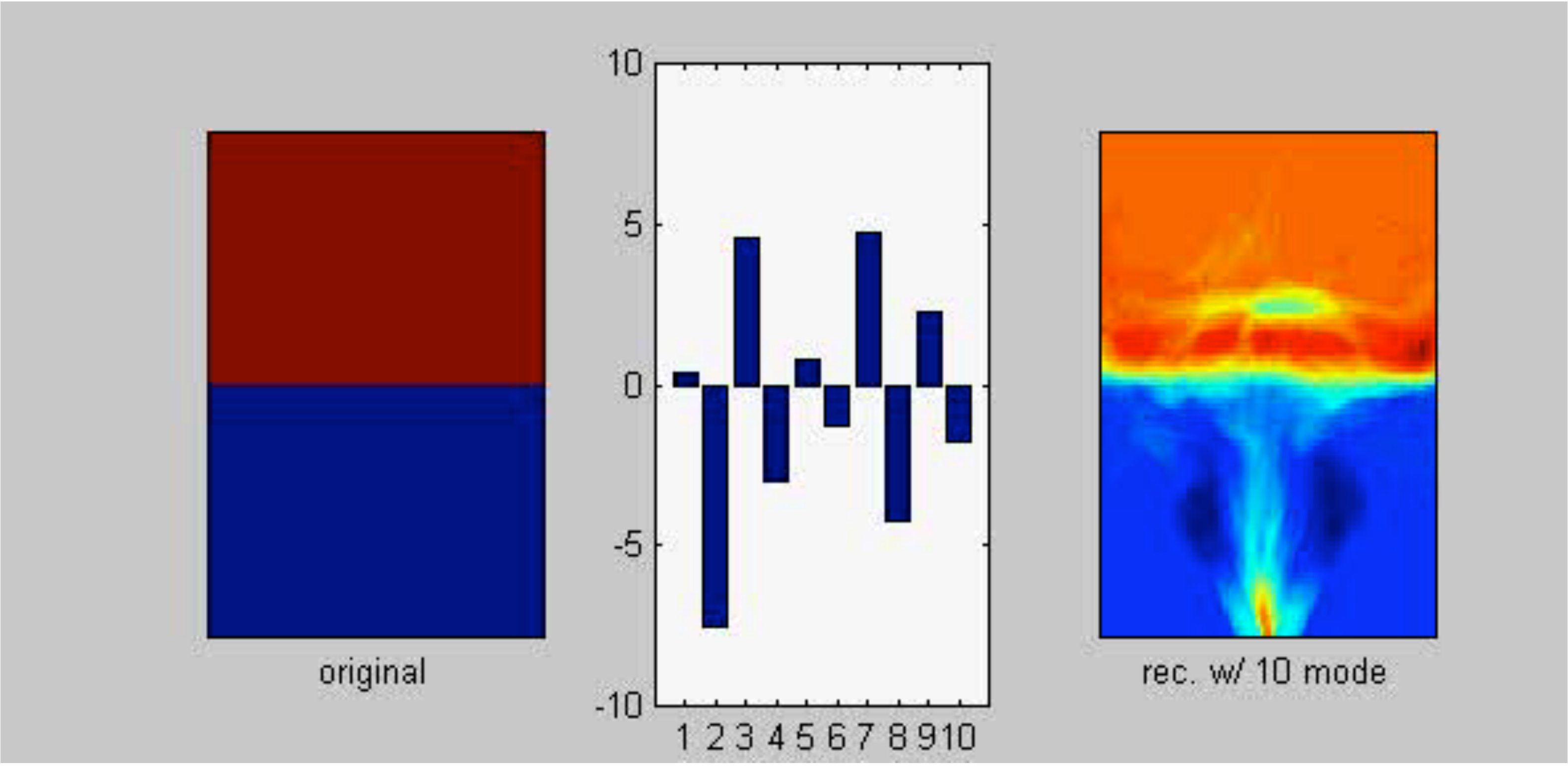

Current Related Research Projects

- DOE
  - A Reduced-Order Model of Transport Phenomena for Power Plant Simulation
- AFOSR
  - Rotating Stall Suppression Using Oscillatory Blowing Actuation on Blades (co-PI: O. Rediniotis)
- AFOSR
  - A Novel Method for the Prediction of Nonlinear Aeroelastic Responses (co-PI: T. Strganac)
- Turbomachinery Research Consortium
  - Prediction of Fluid Instabilities in Hole Pattern and Honeycomb Stator Seals
- AFRL/GUIDE Consortium
  - Turbomachinery Aeroelastic Analysis Using a Continuation/ Proper Orthogonal Decomposition Method

Current Research Team

- Thomas Brenner - Ph.D. (G8)
- David Liliedahl - Ph.D. (G8)
- Forrest Carpenter - Ph.D. (G8)
- Greg Worley - M.S. (G7)
- Will Carter - Ph.D. (G7)
- Raymond Fontenot - M.S. & Ph.D. (G7)
- Robert Brown - UG (G4)

Questions?

Parallel Rotor-Stator Interaction (PaRSI)

- Reynolds-averaged Navier-Stokes quasi-3D solver
- **Features**
  - Finite-difference, structured (multiblock), implicit, parallel, unsteady, with rotating, pitching and plunging blades
- 22,300 code lines
- **Sponsor**: Westinghouse Power Generation
- **Impact**
  - airfoil clocking increased efficiency by up to 2 points
  - clocking is now incorporated in turbomachinery design process

Unsteady Unstructured 3D (UNS3D)

- General Reynolds-averaged Navier-Stokes 3D solver
- **Features**: Control volume, unstructured, explicit, unsteady, multigrid, parallel
- 11,400 code lines
- **Sponsors** (2000-present): Turbomachinery Research Consortium (for internal flows), AFOSR (for external flows and aeroelastic applications)
- **Impact**
  - internal flows: predicted axial loads on centrifugal compressors to prevent bearing failure; fluid instabilities in honeycomb stator seals
  - external flows: predict aerodynamic nonlinearities (shock and flow separation) needed to understand nonlinear fluid-structure interactions

Grid Generator (GG)

- Hybrid (structured/unstructured) 3D grid generator
- **Purpose**
  - allow very large deformation w/out regriding
  - same topology from hub to tip for extreme turning
  - facilitate parallel processing
- **Features**
  - O-grid structured (Poisson solver or conformal map-ping) for viscous region
  - deforming triangular prisms
  - topologically identical layers for parallel processing
- 8281 code lines
- **Sponsors**
  - Turbomachinery Research Consortium & AFOSR (2000-present)

Grid Generator (GG)

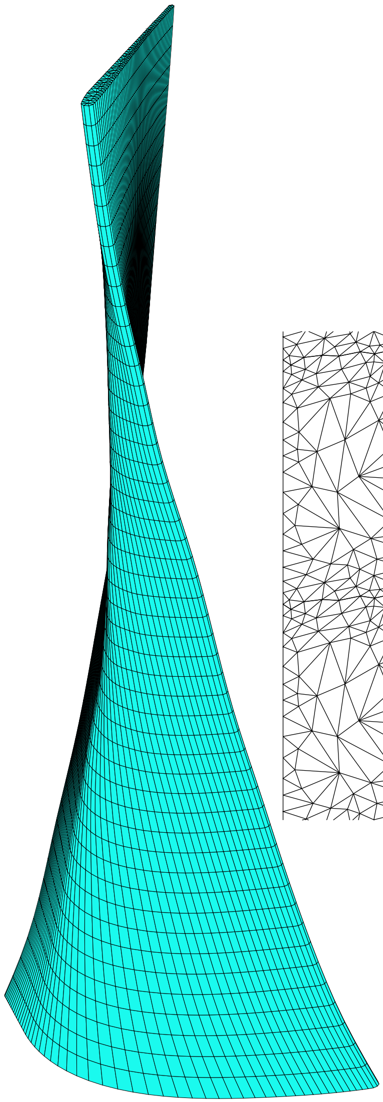

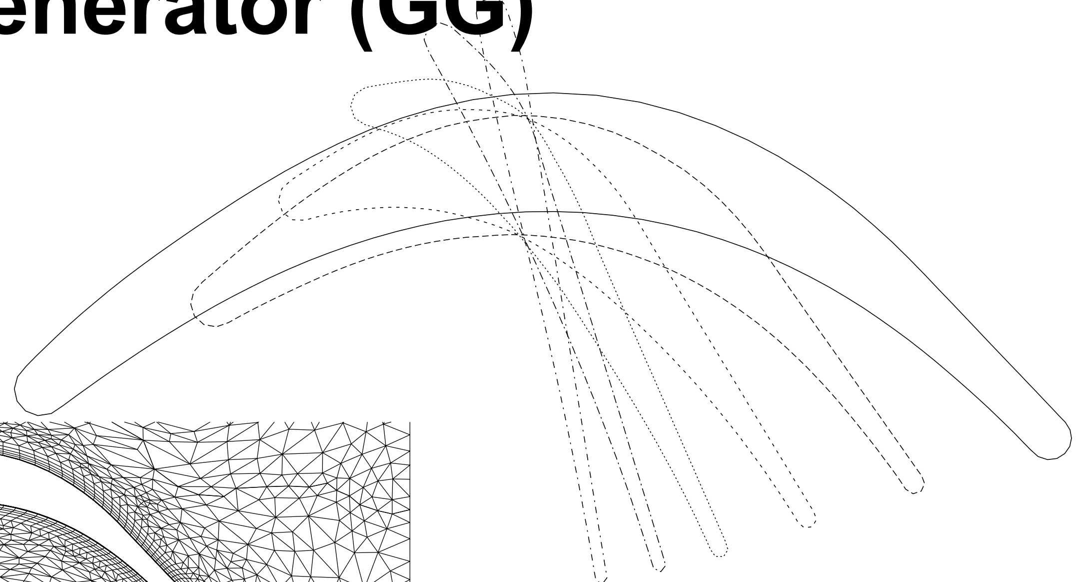

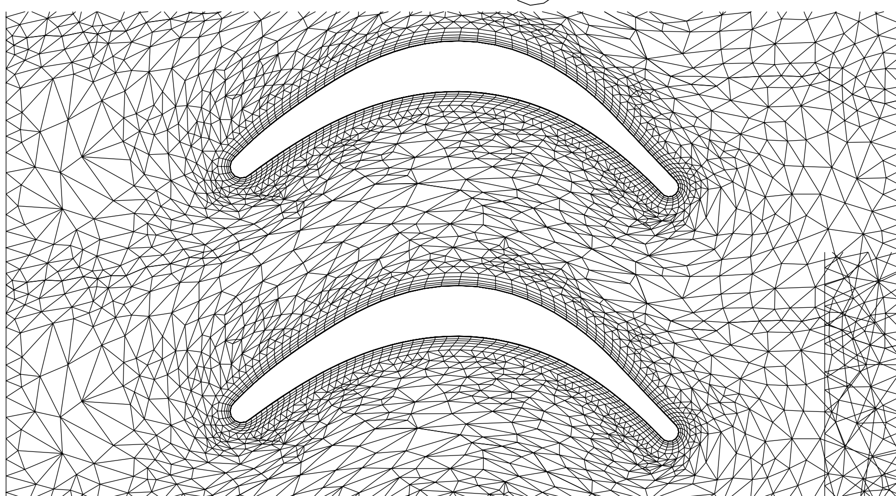

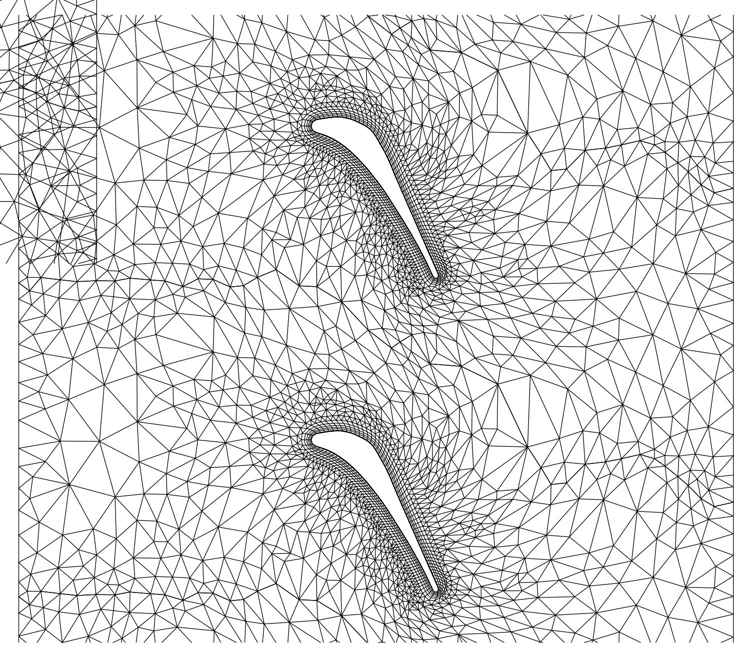

Combustion and Rotor-Stator Interaction (CoRSI)

- Combustion in rotating machinery, based on RANS
- **Features**
  - Finite difference, unsteady, implicit
- 15,600 code lines
- **Sponsors** (2001-present)
  - Westinghouse Science and Technology Center
  - U. S. Department of Energy
  - Siemens (Germany)
- **Impact**
  - Supports development of turbine-combustors, a *“nascent and compelling”* propulsion thrust area (National Research Council’s Committee on Air Force and DoD Aerospace Propulsion Needs)

Nonlinear Aeroelastic Interaction

Motivation

- Evidence of beneficial responses attributed to nonlinearities
  - example: bird flight
- Evidence of adverse responses attributed to nonlinearities (that affect air vehicles)
  - examples:
    - Limit Cycle Oscillation (LCO): F-5, F-15 STOL, F-16, F-111, F/A-18
    - Residual Pitch Oscillation (RPO): B-2

Physical Sources of Nonlinearities

- Structural
  - Geometric structural nonlinearities (ex.: panel flutter)
  - Control surface freeplay
  - Internal structural damping
  - Internal and auto-parametric resonances
- Aerodynamic
  - Flow separation (& intermittent TE separation)
  - Shock motion (& interaction with boundary layer)

Nonlinear Aeroelastic Interaction

A tightly coupled CFD-CSM aeroelastic solver models nonlinear structural and aerodynamic interaction:

- RANS-based Aerodynamic Model
- Nonlinear Structural Model
- Tightly Coupled Solution

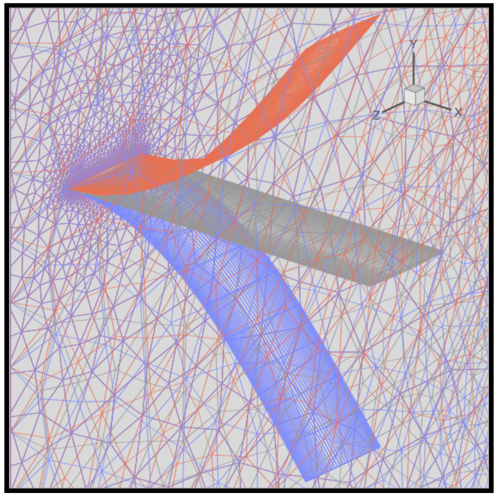

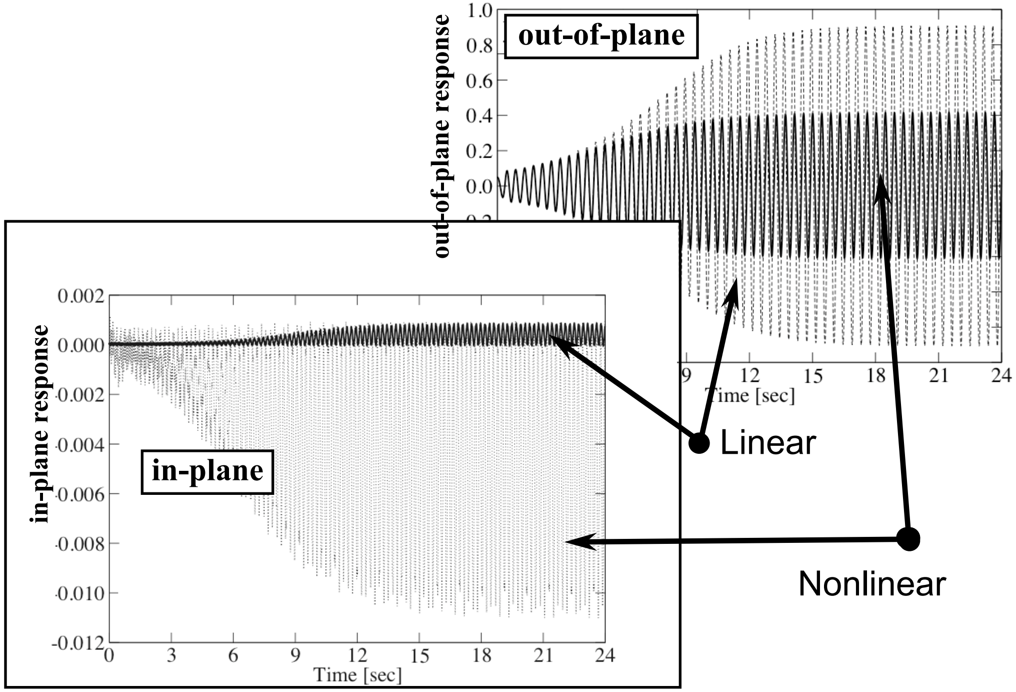

Remarkable in-plane responses arise from nonlinear coupling with out-of-plane bending and torsion

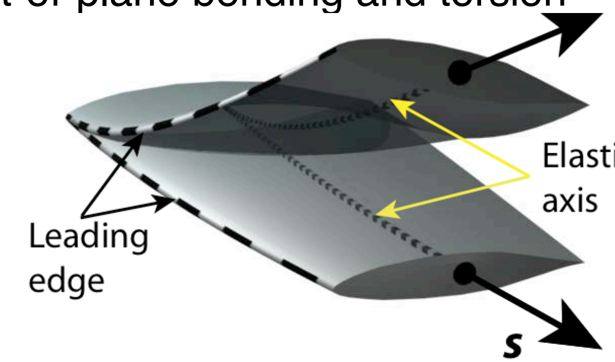

Aeroelastic Model

- Aerodynamics model
  - Reynolds-averaged Navier-Stokes equations
  - Shear stress transport (SST) turbulence model
- Structural model
  - Nonlinear beam (T. Strganac)
    - Nonlinear equations of motion (with quadratic and cubic nonlinearities)
      - In-plane bending
      - Out-of-plane bending
      - Torsion
  - FEM
    - plate elements (Michael McFarland, UIUC)
    - brick elements (John Whitcomb, TAMU)
- Tightly coupled aerodynamics and structural models

Mesh Generation

- Requirements
  - Allow large wing deformations without remeshing
  - Allow a good control of grid size in boundary layer
  - Facilitate parallel computation
- Implementation
  - Layers of topologically identical elements in spanwise direction
  - Structured O-grid around the wing surface
  - Unstructured grid outside of O-grid mesh

Mesh Generation

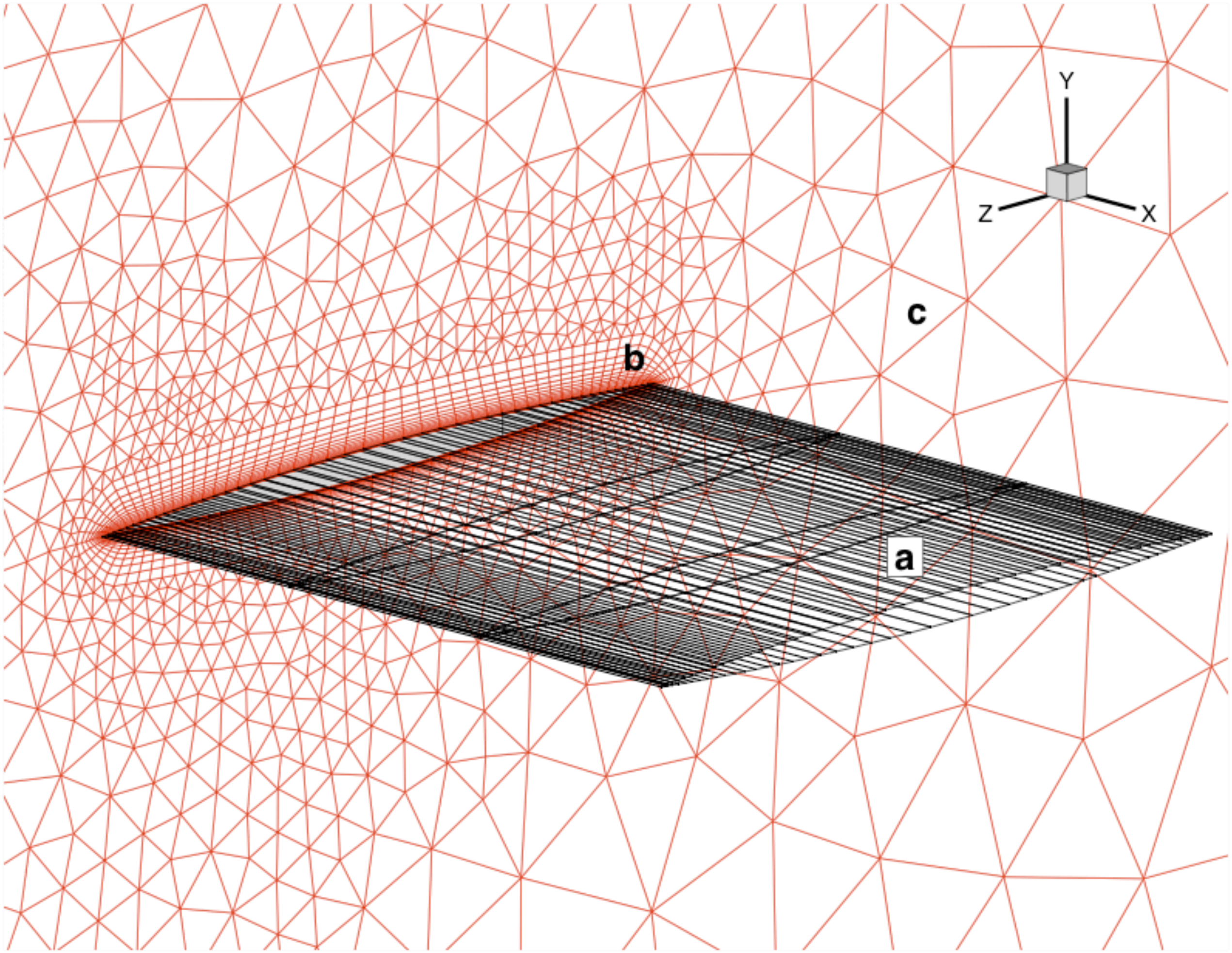

Mesh Generation
O-Grids

Poisson solver

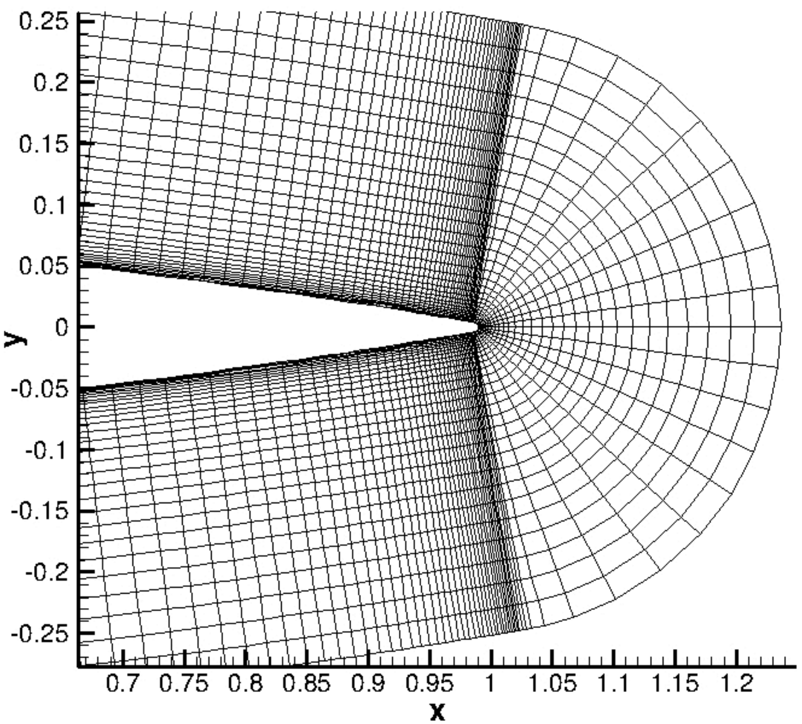

Conformal mapping

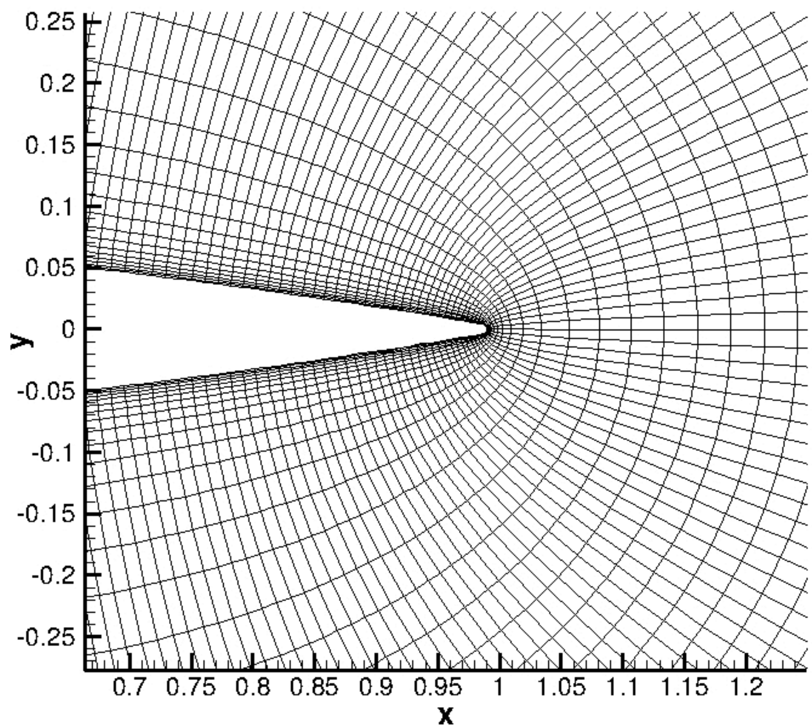

Mesh Deformation

- Deformations
  - elastic axis displacement
  - wing rotation
  - chord-wise bending
- Techniques
  - Spring analogy
  - Conformal mapping
  - Boundary orthogonal layers

Mesh Generation
Chord-wise Deformation

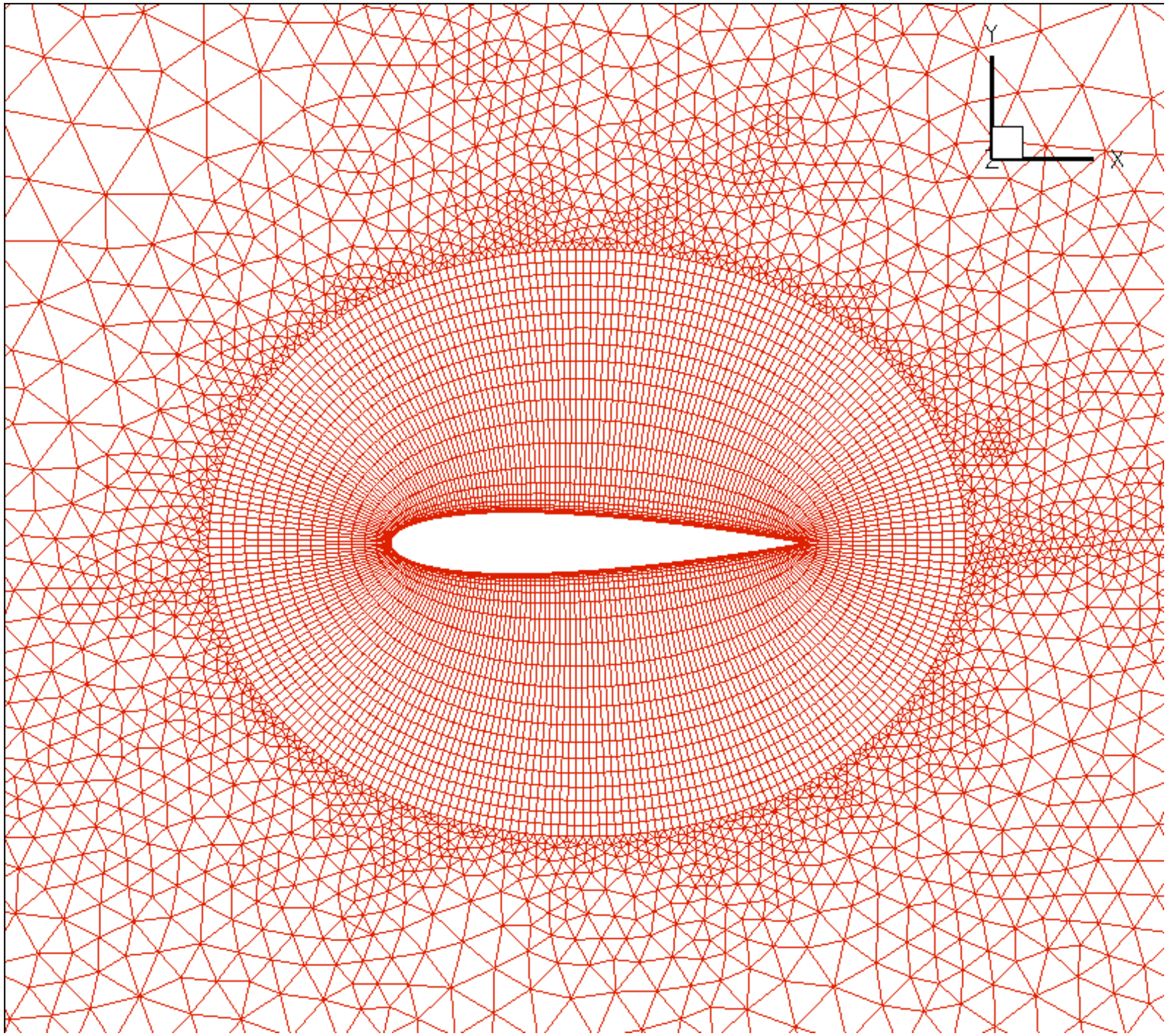

GG - Grid Quality

GG - Grid Quality

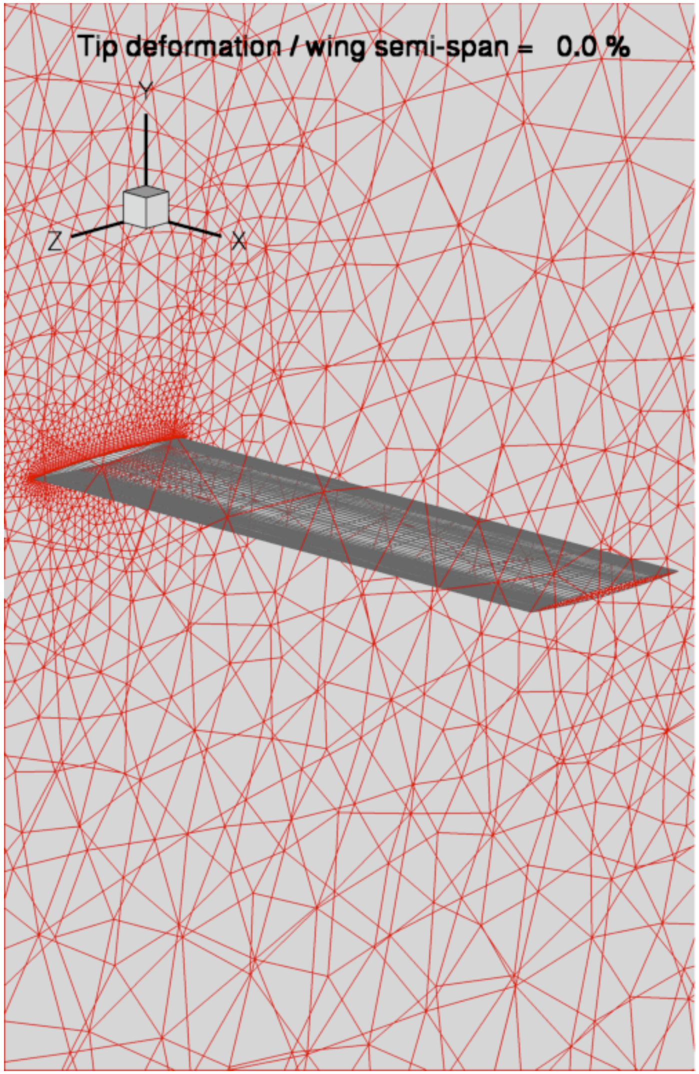

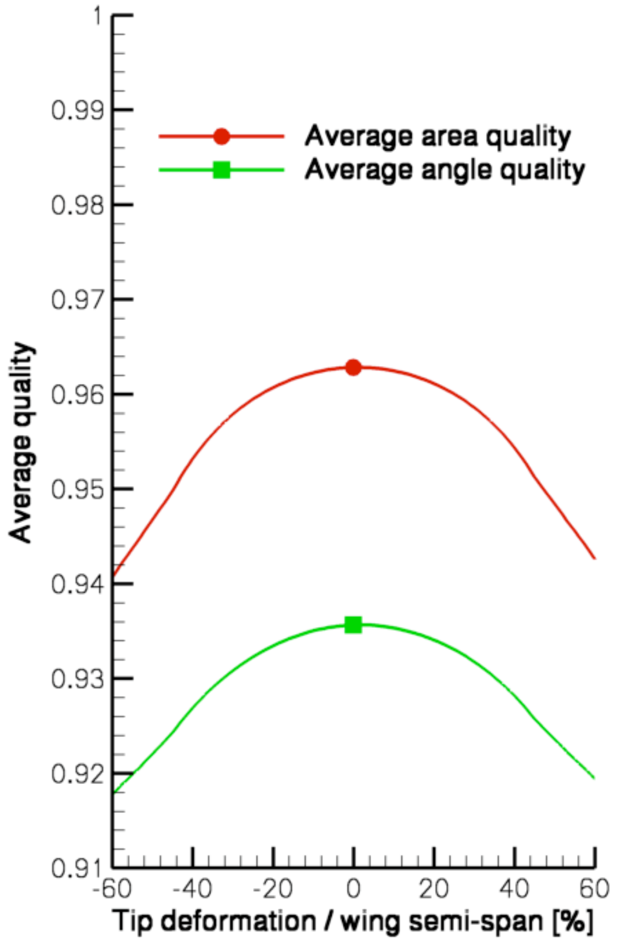

Flow Solver

- Finite volume method
- Dual-mesh cell-vertex method
- Edge-based method
- Upwind method for convective flux
- Least-squares with QR (or Green-Gauss) for gradients
- Piecewise linear reconstruction
- Multi-stage explicit time integration with local time stepping and residual smoothing
- Deforming cell capabilities (using GCL)
- Multigrid
- Parallel computation

F-5 Wing & Transport Jet Wing

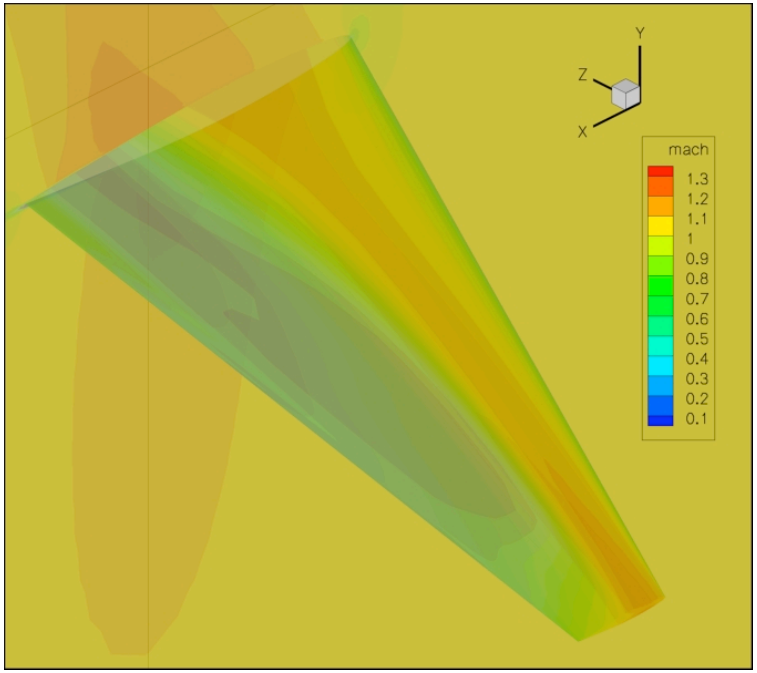

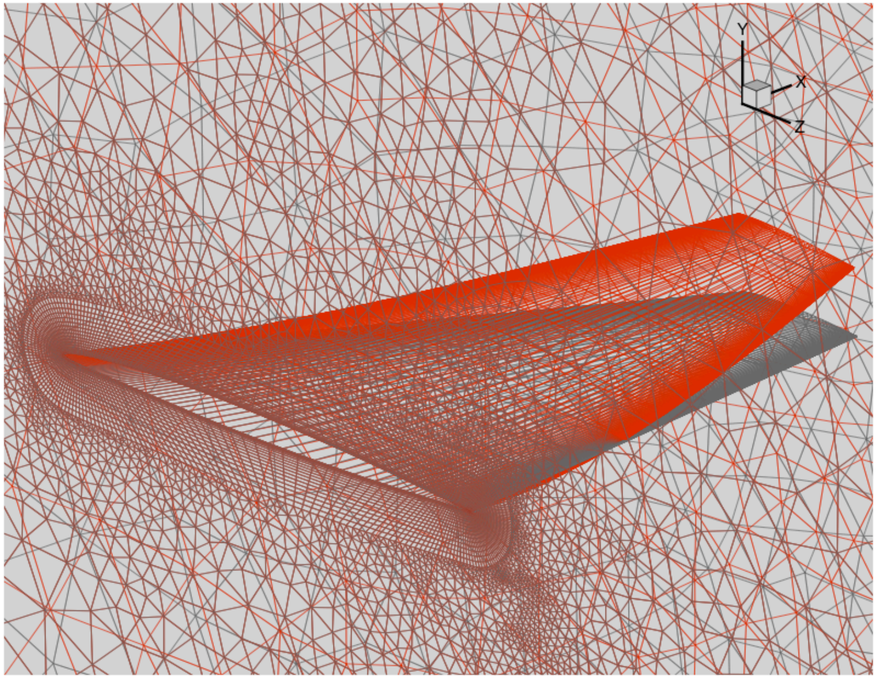

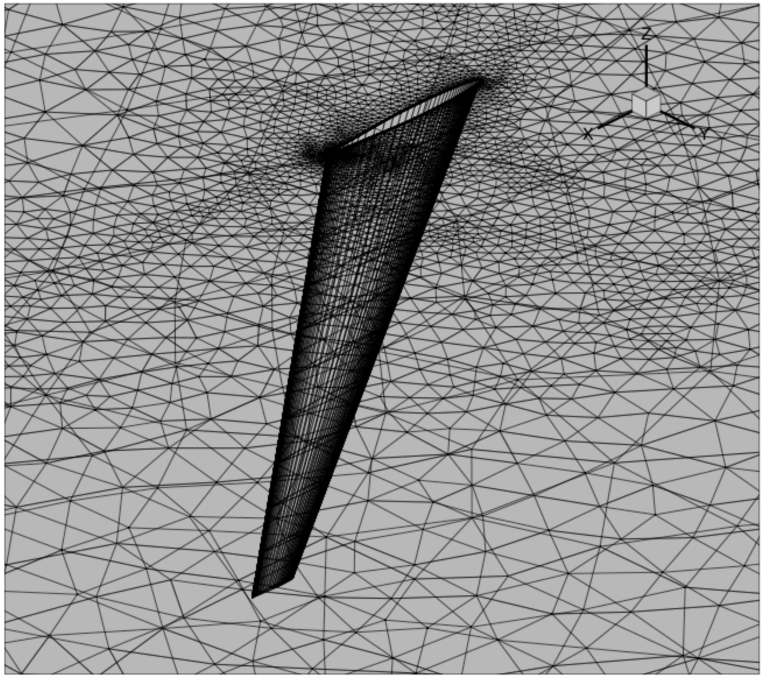

Validation

- Heavy Goland wing at Mach=0.09 (AIAA-2006-2073)
- Heavy Goland wing at Mach=0.7 (AIAA-2006-2073)
- Original Goland wing, stability boundary (IFASD 2007)
- F-5 wing (AIAA-2007-330)
- Nonlinear Aeroelastic Test Apparatus (NATA) wing

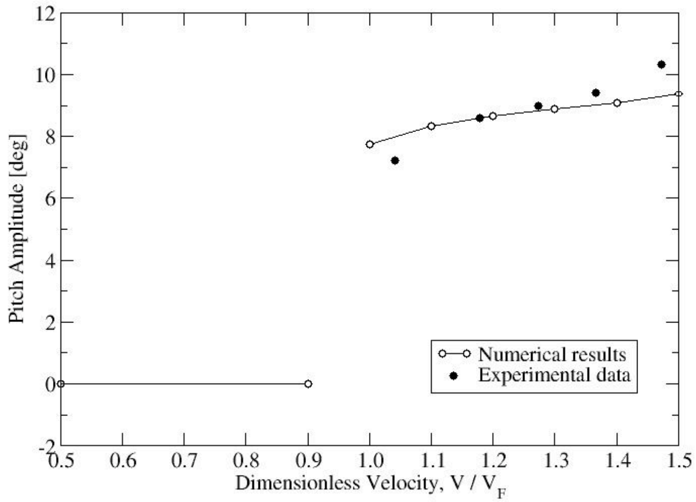

nonlinear pitch
linear plunge

UNS3D - Examples

UNS3D - Examples

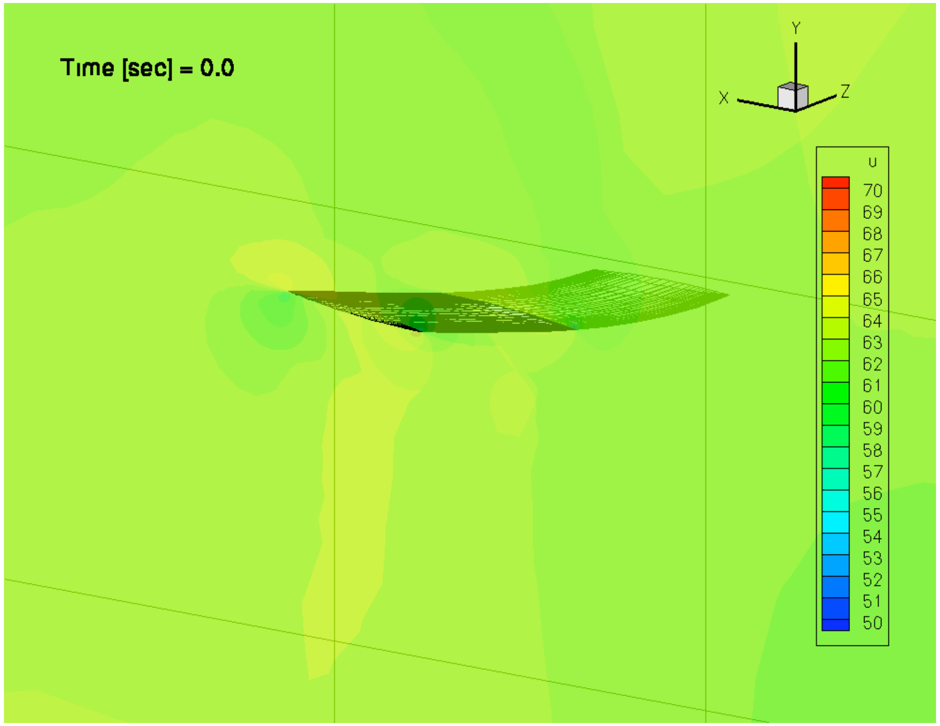

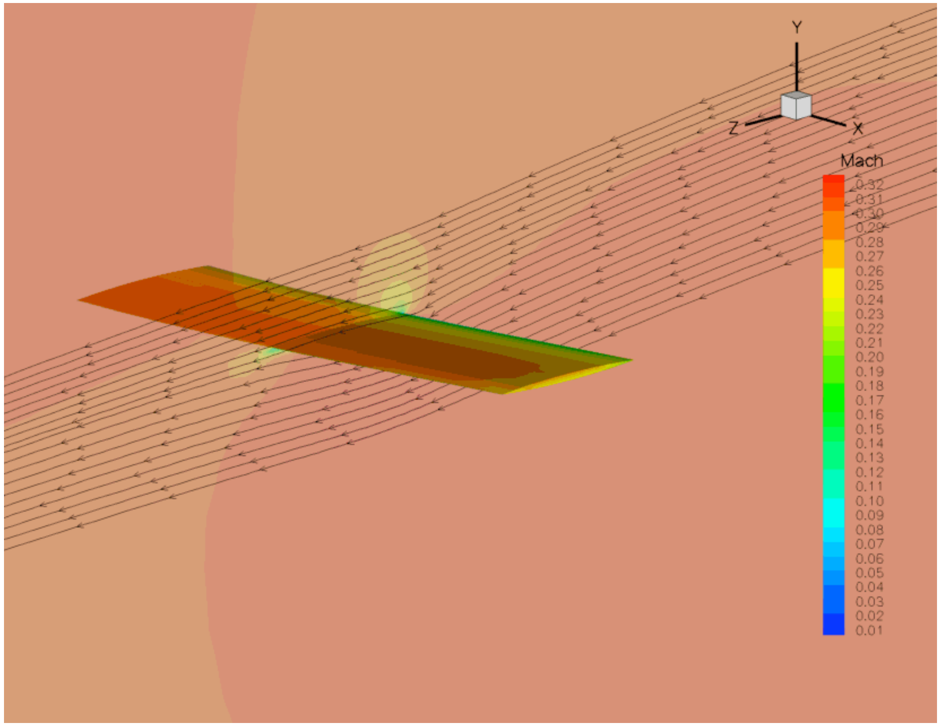

UNS3D - Examples